Norwegian University
of Life Sciences

Master's Thesis 2023 30 ECTS
The Faculty of Environmental Sciences and Natural Resource Management (MINA)

Spatial Optimisation of Offshore Wind in the Norwegian Economic Zone

A Portfolio Approach

Henning Straume
Renewable Energy

Acknowledgements

This thesis marks the end of my master's program in renewable energy at the Norwegian University of Life Sciences.

I would like to thank my supervisor Muyiwa Samuel Adaramola and all professors and lecturers that have given me valuable knowledge in many subjects during eight years of studies. A special thanks to my co-supervisor, Ida Marie Solbrekke, for great support and making the data used for this thesis available.

I would also like to express my gratitude to Daniel Rognes and Jon Eiken for being the best friends and roommates possible during my two bachelor's degrees at the University in Bergen. Additionally, I would like to thank my classmates Martha Johanne Pedersen, Lars Risebrobakken, Eskil Eriksen and Jarand Gaupholm Samnøy for all the support and hours spent together during the process of writing this thesis. I would also like to say thanks to my sister Hanne Marie Straume for being the best proof-reader one could imagine. Lastly, I would like to thank my partner Elisabeth Tran for being there in support and always bringing a smile to my face.

Ås, 15th May 2022
Henning Straume

Abstract

The Norwegian government aims to allocate areas with a potential of 30 GW offshore wind within 2040. Because of the stochastic nature of wind power as a weather-dependent energy source, a more holistic approach to energy planning is needed. The distance across the Norwegian economic zone (NEZ) are vast due to Norway's elongated shape. Thus, NEZ experience many types of weather at the same time. This can cause challenges for the Norwegian power system as wind power can fluctuate quickly. This thesis investigates the characteristics of eight selected offshore sites across NEZ. Data is gathered from a high-resolution offshore wind power dataset called NORA3-WP, which is derived from the meteorological hindcast dataset NORA3. Modern portfolio theory (MPT) is also utilized on all eight sites to determine the optimal spatial distribution of offshore wind in two different scenarios. The eight sites are optimised for the mean-variance and Sharpe-ratio portfolio in both scenarios.

Sammendrag

Den norske regjeringen har som mål å tildele områder med potensial på 30 GW havvind innen 2040. På grunn av den stokastiske naturen til vindkraft som en væravhengig energikilde, er en mer helhetlig tilnærming til energiplanlegging nødvendig. Avstanden på tvers av Norges økonomiske sone (NEZ) er stor på grunn av Norges langstrakte form. Dermed opplever NEZ mange typer vær samtidig. Dette kan føre til utfordringer for det norske kraftsystemet, ettersom vindkraft kan svinge raskt. Denne avhandlingen undersøker egenskapene til åtte utvalgte områder for havvind i NEZ. Data samles inn fra et høyoppløselig offshore vindkraftdatasett kalt NORA3-WP, som er utledet fra det meteorologiske datasettet NORA3. Moderne porteføljeteori (MPT) blir brukt på alle åtte områdene for å bestemme den optimale fordelingen av havvind i to forskjellige scenarier. De åtte havvindområdene er optimalisert for gjennomsnitt-varians og Sharpe-forhold porteføljene for begge scenariene.

Table of contents

Tables and Figures

Abbreviations

NEZ	The Norwegian Economic Zone
MTP	Modern Portfolio Theory
TWh	Terra Watt Hours
MWh	Mega Watt Hours
MW	Mega Watt
GW	Giga Watt
IEA	International Energy Agency
NVE	The Norwegian Water Resources and Energy Directorate
NAO	North Atlantic Oscillation
m.a.s.l.	Meters above sea level
m/s	Meters per second
h	Hour
km	Kilometre

1 Introduction

Global warming is widely regarded as one of the most critical challenges the world faces in the 21st century. With current policies, the world moves toward 2.8˚C temperature rise by the end of the century (UNEP, 2022). This is significantly higher than the international stated goal of the Paris agreement, where global warming was agreed to be limited to a rise of 2˚C, compared to pre-industrial levels. The European Union and Norway have goals of 55% emission reductions within 2030 (European Commision, 2022; Regjeringen, 2022d). To reach their goals, they must efficiently reduce their emissions during the next few years. According to the International Energy Agency (IEA), more than two-thirds of total greenhouse gas emissions originates from the energy sector (IEA, 2021). As 80% of the total global energy supply comes from fossil fuels, a shift towards renewables are needed to fulfil the emission reductions agreed in the Paris Agreement.

Plentiful availability of renewable and cheap hydropower has been Norway's main advantage throughout the 20th century, leading to large-scale industry blossoming with low energy costs. Electricity production in 2021 were 157.1 TWh, while electricity consumption were at 139.7 TWh (Statnett, 2022a). However, an ever-lasting growth in electricity demand combined with few rivers and streams available for hydropower development, puts Norway's energy balance at risk. Statnett estimates a national deficit of 2TWh already in 2027 in their report *Kortsiktig markedsanalyse 2022-27* (Short-term market analysis 2022-27) (Statnett, 2022b). Out of the 5 total Norwegian bidding areas, the three southern areas are estimated to have a combined deficit of 7 TWh. Furthermore, Statnett (2023) estimate in their base scenario that consumption will reach 220 TWh in 2050. With a potential of only 23 TWh increased production from hydropower, solutions with other renewable energy sources are necessary (Henriksen et al., 2020).

Solar and wind power is forecasted to be the dominating electricity producing technologies globally by 2050 (DNV, 2021). Norwegian solar resources are on a global comparison poor. Thereby, the installed capacity in Norway in 2020 were only 160 MW (Energifakta Norge, 2021). In comparison, installed onshore wind were 4 GW the same year (NVE, 2022). Onshore wind development progressed quickly during the end of the 2010s. A growth from almost 900 MW in 2015 to almost 5 GW in 2021 gave an indication that Norway had settled on a way

forward. However, political opinions quickly shifted. Public support for onshore wind in Norway reached an all-time low in 2021, falling from 65% support in 2018 to 33% (Aasen et al., 2022). This combined with the expected energy deficit are among the reasons why the Norwegian government released their plan in 2021 to allocate areas with the potential of 30 GW of offshore wind within 2040 (Regjeringen, 2022c).

A more holistic approach to energy planning is beneficial considering the variable nature of renewable energy sources as well as the size of the Norwegian economic zone (NEZ). Least-cost planning have been the prevailing method for development of new electricity generating facilities for several decades (Awerbuch, 2006). However, this has resulted in non-optimal energy production and higher costs for the transmission system operator and the producers themselves. A possible route to solutions can be through the use of modern portfolio theory (MPT) in energy planning. Taken from finance, MPT is a widely recognized tool for optimising asset diversification and have been used in several analyses for energy planning in the last few decades.

This thesis will evaluate offshore wind resources across NEZ and electricity generating possibilities with IEA's 15 MW reference turbine. Two different portfolio optimisation techniques from MPT will be performed on wind resources in eight carefully selected sites along the Norwegian coastline for 2 scenarios. Thus, creating a rough screening for optimal geographical placement based on production factors.

1.1 Research questions and boundaries

The objective of this thesis is to analyse how offshore wind in NEZ can be optimised utilizing MPT based on geographical weather differences. The aim is to find the optimal combination for wind turbine dispersion across NEZ. Therefore, this thesis will answer the following questions:

- What are key characteristics of offshore wind resources in NEZ?
- How should offshore wind capacity in NEZ be distributed to obtain the minimum variation or maximum units of production for every unit of variation?
- Which areas should be prioritised from the view of power output and its variability when Norway moves forward to develop its offshore wind capacity if all wind farms are of equal size?

This thesis is restricted to NEZ. Therefore, offshore wind farms in other countries' economic zones, especially in the North Sea, are not considered. These areas, if included, probably alters the result of this analysis. This can also be said for other renewable and variable energy sources in Norway and its surrounding countries. However, the most important assumptions for this thesis are:

- Norway is seen as one single electricity bidding area with no transmission losses or bottlenecks.
- All offshore wind farms are connected to Norway's mainland with radials.

1.2 Structure and layout

Chapter 1 presents the aim and societal background for this thesis, together with the scope and research questions. Chapter 2 presents the theoretical background for offshore wind, weather variability and MPT. In the third chapter, the data utilized in this thesis is presented along with the methodology. Chapter 4 and 5 will present the results and discuss the results, respectively. At the end, chapter 6 will present a conclusion and call attention to some aspects that could be further investigated.

2 Theoretical background

2.1 Offshore wind areas in NEZ

In 2010, The Norwegian Water Resources and Energy directorate (NVE) released their first proposed areas for development of offshore wind in Norway (NVE, 2010). The report used a multi-criteria system to perform a rough screening of Norwegian offshore areas suitable for offshore wind. The results were 16 suitable areas, where 4 were deemed suitable for floating wind turbines and 12 for bottom-fixed wind turbines. Continuing this screening, NVE released a strategic impact assessment ranking the 16 areas into three categories of suitability according to techno-economic criteria and conflict of interests (NVE, 2012).

There are many factors that must be considered when evaluating an area for offshore wind. As mentioned, NVE (2010); NVE (2012) uses a multicriteria system to evaluate areas for offshore wind in NEZ. Since the release of NVE's reports in 2010 and 2012, the technology, cost, and political climate surrounding offshore wind have changed drastically. Installed capacity worldwide have changed from around 3 GW in 2010 to 35 GW in 2020 (Bilgili & Alphan, 2022). Turbines have also grown larger, doubling power output from the largest turbines from 6 MW to 12 MW between 2016 and 2020. Suitable water depths for floating wind is now up to 1000 meters (Solbrekke, I. & Sorteberg, A., 2022; World Bank, 2019). Furthermore, the total cost of offshore wind fell 49% between 2011 and 2021 (IRENA, 2022). Thus, many of the first cleared areas in NEZ by NVE may be outdated and thereby not deemed the most suitable anymore.

2.2 Variability and integration of wind power across distances

Huber et al. (2014) assessed power system flexibility in a system containing large amounts of solar and wind energy. They showed that there are three main factors determining what ramping flexibility is needed in a future power system: Share of variable renewables, their mix, and the geographic system size. Recently, the Norwegian transmission system operator, Statnett, warned about a potential system collapse due to the need of being able to respond to changes in the power system on the timescale of milliseconds when operating a power system with variable renewable energy sources (Abelsen, 2023). Thus, new and more modern systems are required, showing that the need for flexibility increases costs.

It is well known that windspeeds and wind power vary with time and space. Integrating wind energy can pose real challenges to the operation of power systems and grid due its variable nature (Cutululis & Sorensen, 2010). Kiviluoma et al. (2016) finds that variability in wind power production decreases with geographical spread. Martin et al. (2015) explains how interconnecting wind farms across large distances reduces the overall variability in the power system. Further, Kiviluoma et al. (2016) finds that the hourly variability in the European union stays within ± 10% of capacity 99% of the time. These are good signs as Katzenstein and Apt (2012) finds that economic costs arise from variability in wind production. As per their research, the total costs arising from the need to stabilize the power system due to variability on the timescale of 15 minutes to 1 hour for 20 wind farms in Texas where $8.73 per MWh in 2008 and $3.90 per MWh in 2009. Katzenstein and Apt (2012) also found that variability costs decrease with higher capacity factors.

Koestler et al. (2020) studied future challenges to the Norwegian and North-European energy grid given a higher share of renewable energy. They found that wind power have high variabilities across Norway due to its elongated shape. The variation from year to year in wind power production is smaller than the variation of Norwegian hydropower production. However, quick reductions in wind power output will be challenging for the power system. Solbrekke et al. (2020) found that interconnecting offshore wind power in NEZ would reduce variability and reduce the risk of hours with zero production.

Using the MERRA2-dataset, Tande (2022) examined the relationship between production from all the offshore wind areas in NVE (2010). According to that analysis, there is almost no correlation between the areas in the North Sea and the areas starting with Frøyabanken and going north. Again, correlation is found also within NEZ, to be decreasing with distance. This result exhibits temporal robustness on hourly, weekly and monthly timescales. However, the most southerly areas in NVE (2010), Sørlige Nordsjø I and II are strongly correlated with other North Sea offshore wind areas like Doggerbank, Horns Rev and Baltic2. This can impose challenges of balancing the Northern European energy grid as mentioned in Koestler et al. (2020).

2.3 Weather systems and variability in NEZ

Weather in the midlatitudes is typically dominated by cyclones and anticyclones, also called extratropical cyclones and anticyclones. Midlatitudes is approximately defined as 30-60˚N and

S, depending on the specific geographical position. These weather systems in the midlatitudes are following the storm tracks, i.e., from North America and across the Atlantic towards Northern Europe (Chang et al., 2002). This is caused by the westerlies, a belt of prevailing wind from west to east, that is present between 40-60˚N in the northern hemisphere (Greatbatch, 2000). According to Lockwood (1987), the greatest atmospheric variability is found in the midlatitudes, approximately 40-70˚N. This region have significant temperature differences (strong thermal gradients), caused by vigorous westerlies from the subtropics culminating with the polar front jet stream. These temperature differences are the main reason for the creation of cyclones in the midlatitudes (BjerknesCentre, 2020). The zone of westerlies is permanently unstable and thus gives rise to a continuous stream of large-scale eddies near the surface, where the cyclonic eddies moves poleward (Lockwood, 1987). Further on Lockwood explains that variable winds converge into low-pressure belts at about 60˚N, called the subpolar low-pressure area. This low-pressure belt hit the Northern European mainland's coastline in Southwestern Norway, with Norway's second largest city, Bergen, located around 60,4˚N (Kartverket, 2023a).

The number and strength of the cyclones following the westerly belt across the North Atlantic and Northern Europe varies from year to year. The single greatest variability factor in the North Atlantic and Northern Europe is called the North Atlantic Oscillation (NAO) (Greatbatch, 2000). In short, NAO is an index measuring how strong the winds in the westerlies are. It is important to note that NAO is not in a permanent state or static. It describes how strong the fluctuations and pressure differences between the average Icelandic low pressure system and the average Azores high pressure system are. The stream of wind that NAO represents is given by a meridional displacement of atmospheric mass over the North Atlantic area (Wanner et al., 2001). As the wind blowing around the Azores high spins clockwise, the wind around the Icelandic low moves anticlockwise. This results in air being compressed between the Azores high and Icelandic low, creating a narrow passage with strong winds.

As mentioned, NAO is the single greatest variability factor in the North Atlantic and Northern Europe. In fact, 31% of the interannual variance in temperature in the Northwest Atlantic, across Europe and downstream over Eurasia can be explained by changes in NAO (Wanner et al., 2001). Generally, NAO is classified within two phases, positive and negative. These phases are shown in Figure 1. The positive NAO phase has a clear Icelandic low and Azores high. This

is associated with stronger westerlies, and thus stronger wind and higher temperature, over the North Atlantic and Northern European continent (Hurrell & Deser, 2010; Wanner et al., 2001). In opposite, the negative NAO phase is characterised by weaker westerlies and lower temperature. Generally, the NAO index is at its highest in winter and lowest in summer (Hurrell & Deser, 2010).

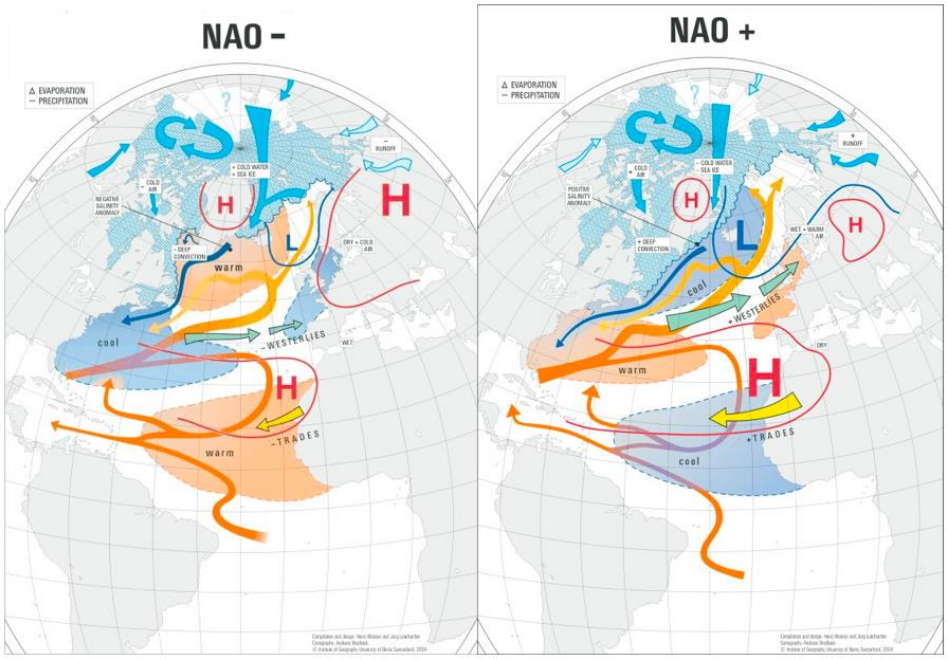

Figure 1: North Atlantic Oscillation negative and positive phase.(OSSfoundation, 2014)

Scandinavian blocking is another weather regime affecting NEZ. Blocking is a weather regime where the prevailing westerlies is blocked due to an anomalous high pressure system (van der Wiel et al., 2019). They are long-lasting, self-sustaining and quasi-stationary systems that occur frequently over certain regions (Kautz et al., 2021). van der Wiel et al. (2019) find that the Scandinavian blocking regime acts as an opposite to the NAO positive phase, with a correlation of -0.68. Occurrence of this regime is known to lower the amount of high wind speeds significantly over the North Sea (van der Wiel et al., 2019). In other areas of NEZ, such as the Norwegian Sea, Scandinavian blocking seems on average to be neutral, while it might bring higher wind speeds to some parts of the Barents Sea.

The fourth weather regime influencing NEZ, is the Atlantic ridge. A negative pressure anomaly over Europe and a positive anomaly over the North Atlantic (van der Wiel et al., 2019). This

regime gives an average occurrence of wind speeds in NEZ and is the least common of the four weather regimes influencing NEZ.

NEZ stretch over a vast distance. The south-western corner located at about 56.09˚N and 3.25˚ E and north-eastern at about 73.38˚N and 36.46˚E (Kartverket, 2023b). This makes up a distance of over 2400 km (GoogleMaps, 2023). Due to the vast distance, NEZ will always experience many types of weather. Cyclones in midlatitudes can grow to be over 1000 km in diameter(Schultz & Vaughan, 2011). Cyclones affecting the Norwegian coastline however, usually never larger than 1000 km in diameter due to it being located at a higher latitude (BjerknesCentre, 2020). These cyclones are thus far smaller than the distance across NEZ. Cyclones travelling from south-west to north-east in the Atlantic have an average propagation velocity of 59 km/h and lifespan of 4.1 days (Gaffney et al., 2007). Wind speeds will also vary within a cyclone, with the top speeds being found right behind the cold front (Schultz & Vaughan, 2011).

Due to the latitudinal extent of NEZ, polar cyclones also occur. These are short-lived and smaller in size than an extratropical cyclone, with a typical diameter of 100-600 km and a common life span of 9-18 hours (Smirnova et al., 2015). Polar cyclones are also quasi-stationary, normally only travelling 100-300 km in its lifetime. In the findings of Smirnova et al. (2015), no polar cyclones have been detected south of Stadt between September 1995 and April 2009.

In summary, NEZ will always experience many types of weather due to vast distances. Given the characteristics of weather in NEZ, offshore wind resources will differ across space and time. To reduce variability, these weather characteristics must be considered, and spatial planning needs to be a part of the process when Norway plans on building offshore wind in NEZ.

2.4 Visual impact and visibility

Wind turbines can be considered as causing visual pollution in several ways. Jensen et al. (2014) argues this includes making the general perception of an area degraded. At the same time, wind turbines adds unnatural movement to the landscape, attracting attention and making the surroundings less peaceful and enjoyable for some. Ólafsdóttir and Sæþórsdóttir (2019) finds that the visual impact of wind turbines for a proposed wind farm in Iceland seems

to be the principal cause of uneasiness among residents. Visual impact are also strongly tied to opposition against development, and ignoring this can lead to a rise of conflict (Rand & Hoen, 2017). Therefore, visibility of an offshore wind park must be considered in governmental planning. Otherwise, public opinion might turn against the future aim of 30 GW offshore wind in NEZ.

Offshore wind turbines are large structures, with IEA's 15 MW reference turbine being 270 meters tall with one blade being perpendicular to the surface it stands on (Gaertner, 2020). The hub height of the wind turbine is set at 150 m.

To find out how far an object like a wind turbine is visible the following formula is used:

$$x = \sqrt{(r+a)^2 - r^2} + \sqrt{(r+b)^2 - r^2},$$

where *r* is the radius of Earth, *a* is the height above sea level for an object, *b* is the height above sea level for an observer, and *x* is the distance between the object and the observer in meters. Visual representation is shown in Figure 2. The formula uses Pythagoras theorem to do a simplified calculation of visibility over the horizon (*H*) from an observer's point of view (*O*) to an object (ob). The volumetric mean radius of earth is given to be 6.371.000 m (NASA, 2021).

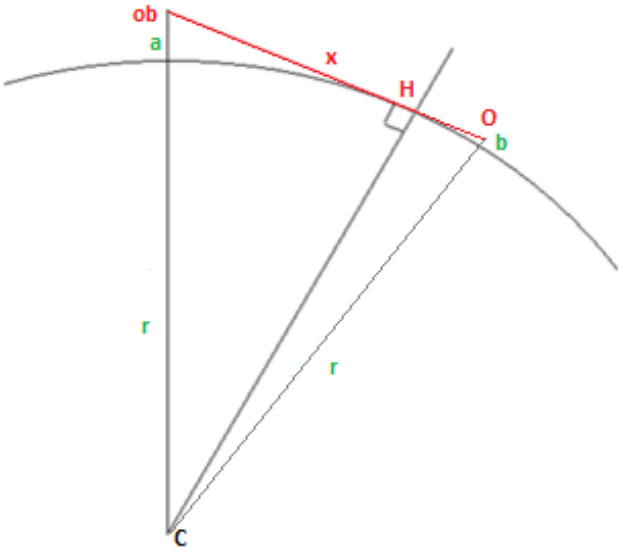

Figure 2: Visual representation of visibility. Made with MS Paint.

Table 1 shows different visibility distances for different heights of the observer and the object. For an observer at sea level, the blades can be visible up to 63.7 km. If the observer stands at a mountain top of 300 m, which is not uncommon in Norway, the blades can be visible up to 120,4 km. However, this is highly unlikely due to meteorological conditions.

Table 1: Calculated maximum visibility distance in perfect meteorological conditions.

Height of observer [m]	Height of object [m]	Distance visible [km]
2	150	48.7
2	270	63.7
150	150	87.4
150	270	102.4
300	150	105.5
300	270	120.4

White Consultants (2020) found in their report *Review and Update of Seascape and Visual buffer study for Offshore wind farms* that East Anglia TWO justifies a visual study area of 50 km, based on analysis of Met Office from Weybourne and Shoeburyness. Visibility over 50 km for these two areas where only possible for 9% of the time in a 10-year period. Results also showed that blade movement for moderately sized wind farms were only visible up to 39 km.

Offshore wind turbines are also required by law to have long-distance lighting installed. Forskrift om rapportering m.m. av luftfartshinder (2014) says that wind turbines in Norway with a height of above 150 meters needs high intensity obstacle lights. These are normally placed on top of the hub. For the IEA's 15 MW reference turbine, the high intensity lights will be located at a height of 150 meters, thus being visible for an observer at sea level for almost 49 km.

2.5 Modern portfolio theory

MPT has its roots in the theory applied by Harry Markowitz in 1952. Markowitz (1952) argued that the sum of the risks of individual assets are higher than the risk of a diversified portfolio. Originally, MPT was used in the financial sector only, but have in the recent decades been used to plan within several sectors, also the energy sector.

2.5.1 From finance to energy

For many years, least-cost planning have been the prevailing way for electricity generating capacity expansion in many countries (Awerbuch, 2006). Simply explained, the least-cost planning method aims to get the most amount of energy from the lowest possible cost. Financial investors know through MPT that a portfolio of assets provides the best means of hedging future risk. Therefore, one would not invest in a single asset based of 20-year forecasted performance. Yet, following the least-cost planning approach, this is what energy producers do (Awerbuch, 2006). Using MPT can therefore give another perspective on how to effectively build a portfolio of electricity generating capacities, both from a private, but also governmental approach.

Several assumptions lies in the framework of MPT. To some extent, these are valid within the financial markets. However, these assumptions are not made for a variable weather and energy system. MPT assume perfect markets and no transaction costs, which can be transferred to an assumption of no bottlenecks and transmission losses in the grid. Returns in MPT are also assumed to be distributed normally. This will not be the case for wind power production, where rated power sets an "artificial" cap to return from the view of a financial asset.

2.5.2 Portfolio optimisation in the energy sector

Portfolio optimisation have been used within the energy sector for a few decades. Awerbuch and Berger (2003) used the mean-variance portfolio approach to optimise the European energy sector from a cost-perspective. An optimal investment portfolio in Spanish renewable energy with the focus of monetary risk and return were also made by Muñoz et al. (2009). deLlano-Paz et al. (2017) performed an exhausting review of the literature surrounding application of MPT, confirming that MPT have been widely accepted and proved useful by several studies.

Rombauts et al. (2011) optimise wind-power allocation toward the lowest risk, where goals of specified production across three imagined countries are set and an efficient frontier was created. They developed a method suitable for infinite, none and restricted transmission capacity between the three countries. Roques et al. (2010) looked at five European countries and evaluated optimal placement of wind farms using the mean-variance portfolio. Results

showed that there could be large benefits in a more coordinated European renewable deployment policy.

Reichenberg et al. (2017) analysed if it is possible to distribute wind farms, such that the frequency of low outputs are reduced. Using a multicriteria system, where variability were minimized and production maximized, they concluded that geographic diversification can substantially reduce the risks and instances of low aggregate output. Drake and Hubacek (2007) used portfolio theory to investigate the effect of splitting up a single 2.7 GW wind power farm into four different locations in the UK. They found that optimal dispersion of wind turbines could reduce variability by 36%, while also finding which portfolio dispersion that gave the most units of production per unit of risk.

2.5.3 Sharpe Ratio

The Sharpe ratio is a common measure to evaluate the risk-adjusted performance of a portfolio. Developed by Sharpe (1963), it has become commonly used in portfolio management in the financial sector, but also in research and energy planning (deLlano-Paz et al., 2017). Sharpe ratio S_P can be expressed as:

$$S_P = \frac{r_p - r_f}{\sigma}$$

Where r_p is the expected return of the portfolio, r_f is the risk-free rate, and σ is the standard deviation of r_p

The risk-free rate is the expected return of an investment bearing no risk, i.e., a treasury bond. However, this is a theoretical measure as all investments carry even some small amount of risk. Since power output carries inherent risks that are not shared with financial investments, it may not be appropriate to use the risk-free rate as a benchmark for measuring risk and return. Therefore, when analysing the performance of a portfolio consisting of power output, the risk-free rate is not relevant and is thus excluded from the Sharpe-ratio. The resulting Sharpe-ratio S_P is then expressed as:

$$S_P = \frac{r_p}{\sigma}$$

2.5.4 Mean-variance

The mean-variance approach minimizes the variance of all the assets in a portfolio. Since this approach minimizes the risk in the portfolio, any portfolio giving a lower return than the minimum variance portfolio should never be accepted (Clarke et al., 2010).

2.5.5 The Efficient frontier

The efficient frontier is a set of optimal portfolios that offer the lowest risk for a given level of production. It was introduced by Markowitz (1952) and have until today been substantial in portfolio optimisation. Portfolios not on the efficient frontier is seen as sub-optimal and should never be picked over a portfolio on the efficient frontier.

3 Data and methodology

This chapter describes which data and method that have been used in this thesis. Due to a significant amount of data, everything was downloaded onto an external hard disk for further processing. Several scripts have been run in Python and Matlab, while Microsoft Excel also have been used for data processing. All scripts can be found in the Appendix section.

3.1 Wind resource and power production data - NORA3-WP

Wind resource and power production data in this thesis are collected from the NORA3-WP dataset, created by Solbrekke, I. M. and Sorteberg, A. (2022). NORA3-WP is a publicly available dataset, that is derived from the 3-km Norwegian reanalysis (NORA3) mesoscale-permitting atmospheric hindcast (Haakenstad et al., 2021)**.** According to Haakenstad et al. (2021) NORA3 is a much more realistic weather model both over ocean and in complex terrain. Solbrekke et al. (2021) also show that modelled average wind speeds from NORA3 outperforms ERA5 for all seasons at all sites considered in the study.

NORA3-WP contains statistical data stored for 7 wind resource and 18 wind power related variables for 3 selected turbines, covering the oceans surrounding Norway. This includes the North and Baltic Sea as well as parts of the Norwegian and Barents Sea. Power generation in NORA3-WP are estimated using power curves for three different wind turbines with 6, 10 and 15 MW installed capacity. The three turbines are as following:

- SWT-6.0-154
- DTU-10.0-RWT
- IEA-15-240-RWT

The respective hub heights are 101, 119 and 150m.a.s.l. Monthly data from 1996 up to 2019 are available for all variables, while hourly data in the same period are available only for wind speed and power generation. Variables are available on a horizontal grid with 3x3 km resolution. Monthly windspeed and hourly wind power generation are utilized in this thesis.

3.2 Area coordinates and suitability data

In the process of choosing sites for analysis in this thesis, coordinates from already designated areas were obtained from Regjeringen (2022a); Regjeringen (2022b) and Equinor (2019). Suitability scores in Solbrekke, I. and Sorteberg, A. (2022) were utilized to determine further

sites. The suitability score is a way to measure how well an area meets a set of criteria. Data from fishing and shipping activity, ocean depth, capacity factor, protected areas, distance to major ports and distance to central electrical networks are factors that determine the final suitability score for a given area in NEZ. Thus, conflict of interests and several techno-economic factors are in the underlaying data for this thesis.

The suitability dataset consists of two-dimensional positional data, that align with the positional data in the variables of NORA3-WP. When selecting sites, only those that are deemed technically feasible and have suitability scores placing them within the top 40% of suitable areas are available for selection.

3.3 Site selection

As this thesis aims to look at spatial planning for NEZ, areas along the entire Norwegian coastline had to be evaluated. NEZ have been split into 4 different zones, visualised in Figure 6. South, west, mid and north, with each region having two sites for analysis. The selection of points within each region has been made to ensure spatial distribution. Already established offshore wind areas in NEZ have been prioritised when choosing sites. The selection method is described in the following sections.

3.3.1 Selection of pre-designated areas

Areas already designated for offshore wind in Norway before 1. January 2023 were chosen. These include Sørlige Nordsjø II, Utsira Nord and Hywind Tampen. Sørlige Nordsjø II is one of two sites in the southern region, while Utsira Nord and Hywind Tampen makes up the two sites in the western region. Therefore, one more site is needed for south, and two sites are needed for mid and north. Utsira Nord and Hywind Tampen are rectangles, and thus, the midpoint was calculated using the average of the coordinates. Sørlige Nordsjø II is, however, in the shape of a pentagon. As Figure 3 shows, Sørlige Nordsjø II still resembles a rectangle. Thus, the midpoint was calculated in the same way as for Utsira Nord and Hywind Tampen, using the four corners visible in Figure 3.

Figure 3: Map showing the area designated for Sørlige Nordsjø II. Northern Denmark and Southern Norway for reference. Made with Python. Zoomed in version of script in appendix D.

The midpoint coordinates for the three areas were then used in the script shown in Appendix A to find the closest point in the NORA3-WP dataset. In this script, Euclidian distance were used to calculate the shortest distance to a point in the dataset. The resulting datapoints in NORA3-WP where then reversed to find the exact location of the datapoints in the dataset. This was done by using the script in Appendix B.

3.3.2 Selection of non-designated areas

To facilitate the selection of non-designated areas, data provided from Solbrekke, I. and Sorteberg, A. (2022) were utilized. A Matlab-file containing the position of areas that received a suitability score of 4 or 5 out of 5 was processed using the script in Appendix C. Figure 4 display these areas with a blue dot.

Among the areas that received a sufficient suitability score, individual points were identified, with an emphasis on spatial distance and whether they were located within a cluster of points. Furthermore, with the reasoning given in section 2.4, a minimum distance of 50 km from mainland Norway was included in the selection process. The minimum distance was also considered due to the higher occurrence of wildlife near shore compared to remote areas of the ocean.

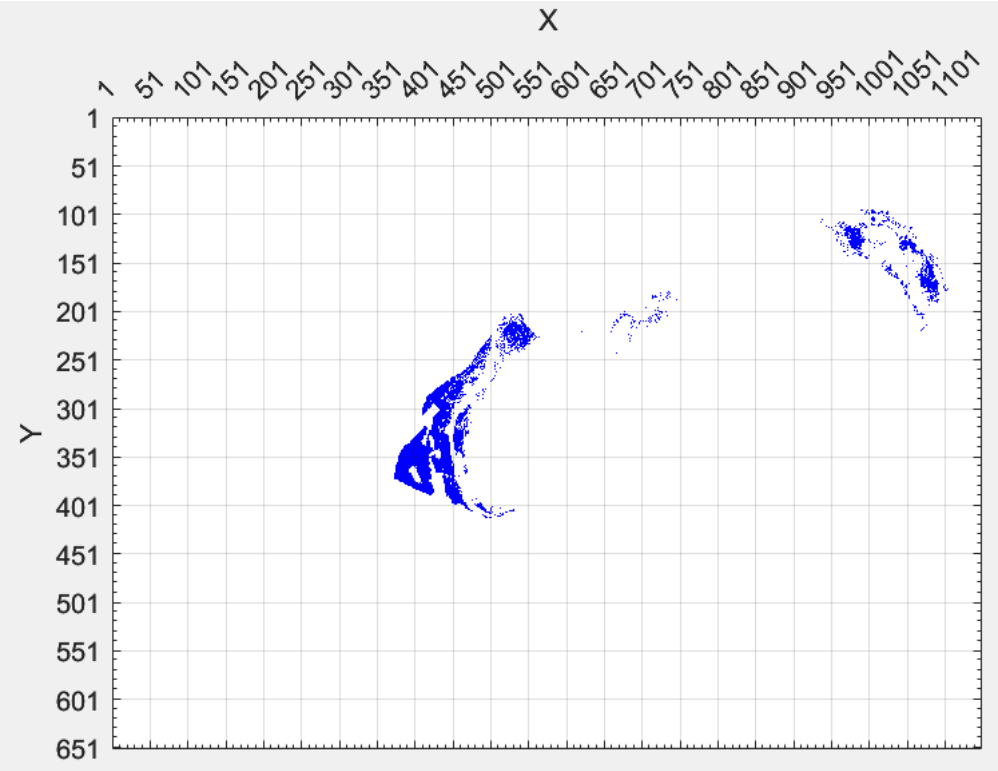

Figure 4: Blue points showing the areas in NEZ which is in the top 40% of suitability for offshore wind according to Solbrekke, I. and Sorteberg, A. (2022). Made in Matlab.

A single point represents only a 3x3 km area, and as such, it is not suitable for offshore wind parks unless it is surrounded by other suitable points. Latitudinal and longitudinal location of the non-designated selected sites were found using the script provided in Appendix B.

3.4 Data compounding and portfolio set-up

Power output for each selected site was extracted using the python script in Appendix E, while windspeeds was extracted using the python script in Appendix F**.** Wind turbines, especially for offshore wind farms, continue to grow and turbines with 15 MW installed capacity are already far into development. Therefore, giving the time-scope of Norwegian offshore wind, production for IEA's 15 MW reference turbine was extracted. Therefore, windspeeds at 150 m.a.s.l were used for the data throughout this thesis, as future offshore wind turbines are predicted to get even larger than those being installed today. The results of the data extraction using the python script in Appendix E are a matrix with dimensions 210834 x 9. This matrix includes a time column and hourly production for each site from 1. Jan 1996 to 31. Dec 2019. The script transferred this matrix into an Excel-file where portfolio optimisation was performed. Additionally, a correlation matrix was also made separately in excel.

To optimise the portfolio, the "what-if analysis" add-in program Solver in excel was used. The optimisation was carried out using an 8x8 covariance matrix and production data for each site. The portfolio's output is the weighted average production in MW, portfolio variance, portfolio standard deviation and Sharpe-ratio. Weighted average production, P_p is calculated by:

$$P_p = \sum w_i P_i$$

Here w_i is the weight of site *i* in the portfolio and P_i is the average production for site *i* in the span of the 24 years NORA3-WP covers. The portfolio variance σ_p^2 is given by

$$\sigma_p^2 = \sum_{i=1}^{n} \sum_{j=1}^{n} w_i w_j cov(P_i, P_j)$$

Where w_i and w_j are the weights and $cov(P_i,P_j)$ is the covariance of production from site *i* and *j*. The covariance matrix used in the calculations can be found in Appendix G**.** As explained above in section 2.5.3 the Sharpe-ratio is expressed as:

$$S_p = \frac{r_p}{\sigma}$$

3.5 Scenarios

Two scenarios have been analysed. In the first scenario, the portfolio must find the optimal placement under the restrictions of:

$$0 \leq w_i \leq 0.25$$

This indicates that no site can have more than 25% of all the offshore wind in NEZ. This restriction was imposed to account for short and long-range wake effects and to ensure the feasibility of the selected capacity in each area. An efficient frontier was generated for this scenario. To create the efficient frontier, minimization of portfolio-variance have been undertaken for several targets of production to make the efficient frontier.

In the second scenario, the portfolio can only select one and one site, and thus must find the optimal placement under the restrictions of:

$$w_i \in \{0,1\}$$

The rationale for this is that building more offshore wind farms in an area where development has already started tends to be more cost-effective. At the same time, the Norwegian grid needs to be further developed so it can integrate large offshore wind farms. This will require

time, effort and monetary funding. Therefore, knowing which areas to build first would be beneficial. This scenario will be carried out for 1 up to 8 sites being equally developed, providing insights into the optimal order in which to build offshore wind parks in NEZ.

4 Results

4.1 Sites selected

The selection of the eight sites for this thesis is displayed in Figure 5, while Figure 6 provides a visual map representation. The Barents Sea contained two big clusters of suitable areas, one in east and one in the western part. Thus, the process of selecting sites for the northern region was straightforward.

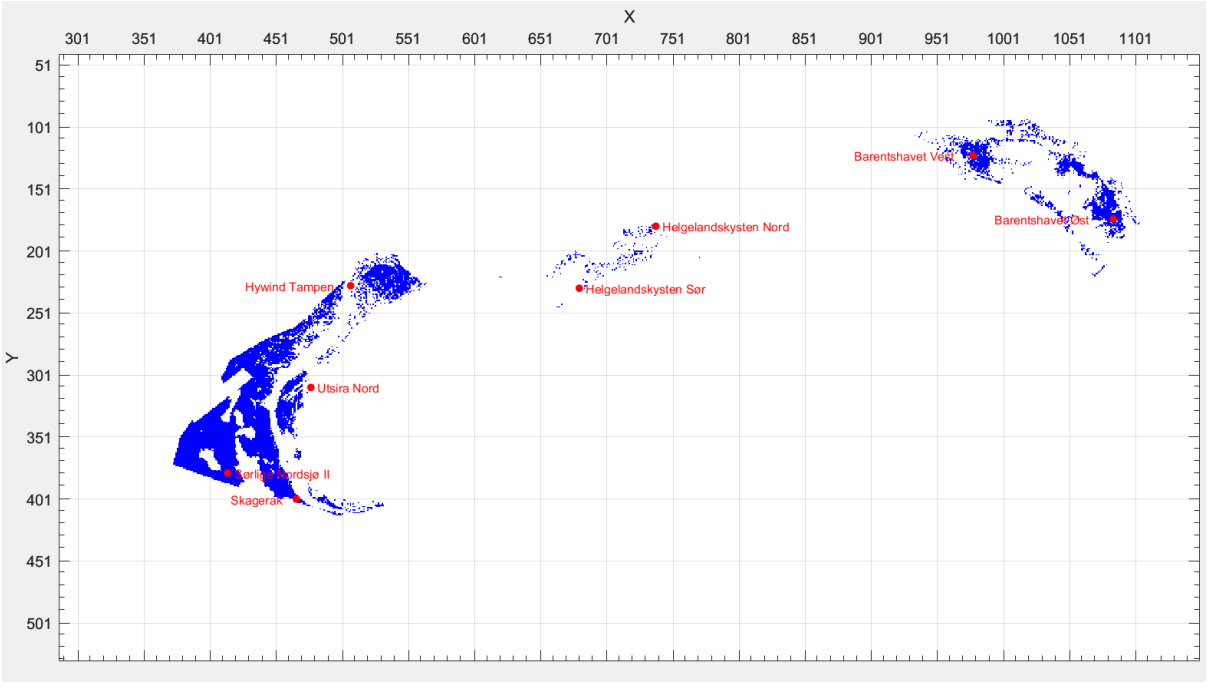

Figure 5: Selected sites for analysis in this thesis. Created in Matlab.

In the case of the mid region, which covers most parts of the Norwegian Sea, points of suitability were scarce, resulting in the absence of significant clusters. Consequently, spatial distance were given a greater weight to provide a more comprehensive understanding of the region's production potential from south to north.

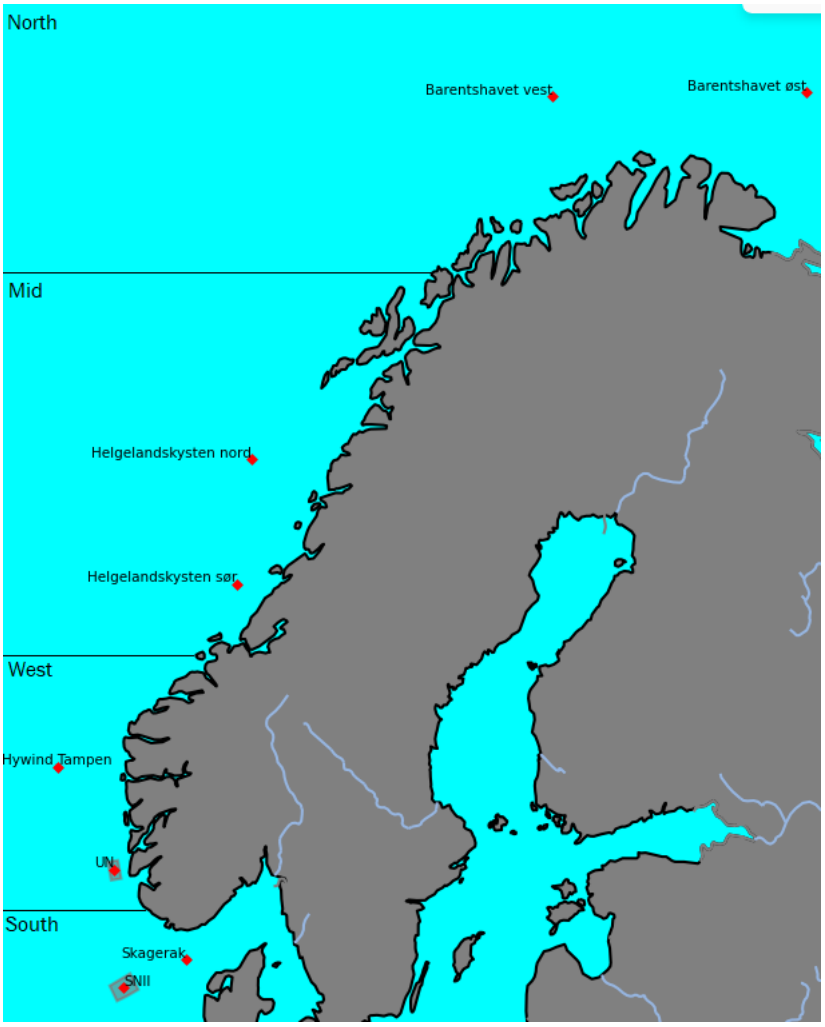

Figure 6: Visual representation of the eight analysed sites and each of the four regions. Grey areas represent the already designated areas for offshore wind by the Norwegian government. Made with Python, script in appendix D.

Skagerak is the last remaining site that was chosen. Situated in the far east of a long arm of suitable points. The selection of the specific point was based on its spatial distance from Sørlige Nordsjø II, as well as its location being more than 50 km away from shore.

4.2 Characteristics of the analysed sites

Table 2 provides both real-world and Matlab-dataset coordinates for each selected site, along with the distance from the shore for each site. The two sites furthest away from each other have over 2.000 km between them. Only Utsira Nord is located within 50 km from the shore, caused by it being a preselected site. The remaining sites range from Helgelandskysten Sør being 56 km away from shore, to Sørlige Nordsjø II being 178 km from shore.

Table 2: Real coordinates, dataset coordinates (X&Y) and distance from mainland's shore for the selected sites in this thesis

Region	Site	Longitude	Latitude	X	Y	Distance from shore [km]
South	Skagerak	7.416	57.390	466	401	65
	Sørlige Nordsjø II	4.890	56.783	414	380	178
West	Utsira Nord	4.502	59.271	477	311	39
	Hywind Tampen	2.244	61.334	507	229	143
Mid	Helgelandskysten Sør	9.451	64.663	680	231	56
	Helgelandskysten Nord	10.029	66.716	738	181	133
North	Barentshavet Vest	22.072	71.844	978	124	127
	Barentshavet Øst	32.229	71.899	1084	175	153

Table 3 displays that all sites have favourable wind resources, leading to capacity factors ranging from 54.7 to 66% before any losses. The average yearly zero hours range from 477 to 800 hours, while the hours of maximum production are between 3187 and 4278 hours. There is a clear geographic trend where the four sites south of Stadt are the top four individual sites for power output.

Table 3: Standard deviation and average characteristics such as windspeed, power output, capacity factor, zero hours and hours of maximum production per year for each site.

Site	Average windspeed [m/s]	Average power output [MW]	Average capacity factor [%]	Standard deviation of production [MW]	Average yearly zero hours [h]	Average hours of max production per year [h]
Barentshavet Øst	9.50	8.67	57.8	6.04	616.3	3349.9
Barentshavet vest	9.44	8.41	56.1	6.12	702.8	3263.1
Helgelandskysten Nord	9.81	8.65	57.7	6.12	688.6	3445.2
Helgelandskysten Sør	9.46	8.20	54.7	6.16	800.1	3187.6
Hywind Tampen	10.67	9.26	61.7	6.16	690.8	3992.5
Utsira Nord	10.23	8.95	59.7	6.20	758.8	3778.0
Sørlige Nordsjø II	10.64	9.79	65.2	5.89	476.5	4128.8
Skagerak	10.71	9.89	66.0	5.92	499.3	4278.1

Figure 7 illustrates the power output profile for each site, which are all skewed towards low values and 15 MW power output. Thus, the power output from the individual sites are not normally distributed. However, as shown in Figure 8 the average power output for all sites

combined for every hour between 1996-2019 appears to be normally distributed. This suggests that as more offshore wind farms are developed, the power output will become more stable around a mean and less skewed than what Figure 7 might imply.

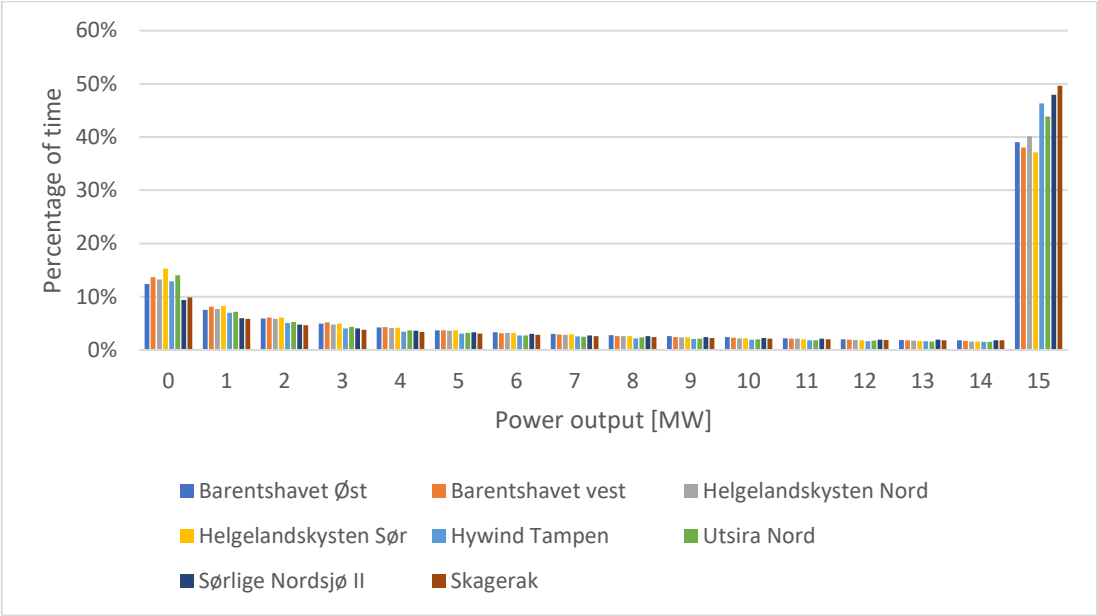

Figure 7: shows how much of the time between 1996-2019 a specific power output have occurred for each individual site. Rounded to nearest integer.

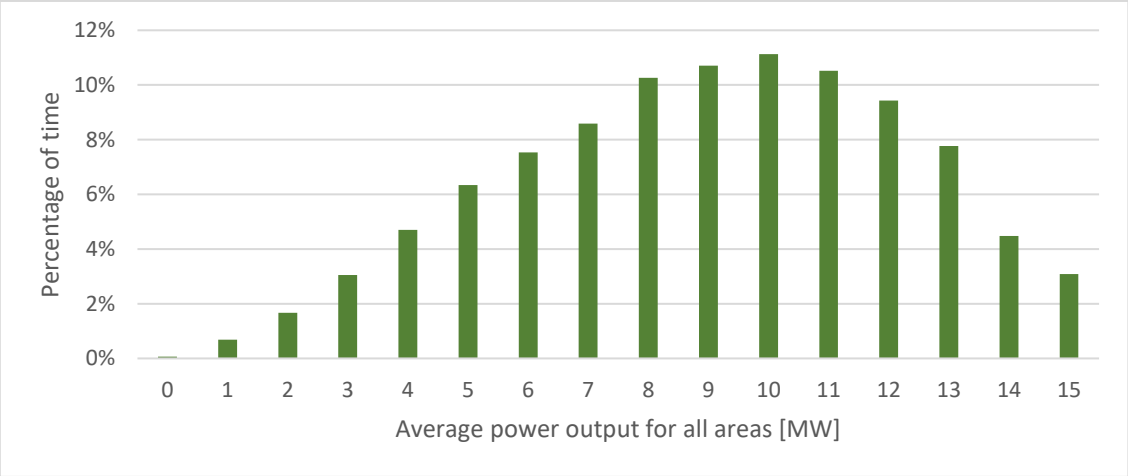

Figure 8: Shows how much of the time between 1996-2019 the average power output for all sites have occurred. Rounded to nearest integer.

4.3 Correlation

Table 4 presents the hourly correlation coefficients between every site in this thesis. It is observed that sites located in the same region have higher correlation coefficients than those located in different regions. Sørlige Nordsjø II and Utsira Nord are the two sites being in different regions with the clearly highest hourly correlation coefficient. The sites in the Barents

Sea exhibit weaker correlations with sites in other regions. Therefore, geographic distance seems to be the primary factor for correlation.

Table 4: Correlation matrix for all sites with the sum of the total correlation for each site.

	BØ	BV	HN	HS	HT	UN	SNII	SG	Sum
Barentshavet Øst (BØ)	1.00	0.31	0.09	0.08	0.05	0.04	0.04	0.03	1.64
Barentshavet Vest (BV)	0.31	1.00	0.13	0.09	0.04	0.02	0.03	0.03	1.66
Helgelandskysten Nord (HN)	0.09	0.13	1.00	0.56	0.22	0.15	0.09	0.09	2.33
Helgelandskysten Sør (HS)	0.08	0.09	0.56	1.00	0.25	0.18	0.10	0.13	2.38
Hywind Tampen (HT)	0.05	0.04	0.22	0.25	1.00	0.47	0.25	0.18	2.46
Utsira Nord (UN)	0.04	0.02	0.15	0.18	0.47	1.00	0.54	0.35	2.75
Sørlige Nordsjø II (SNII)	0.04	0.03	0.09	0.10	0.25	0.54	1.00	0.56	2.62
Skagerak (SG)	0.03	0.03	0.09	0.13	0.18	0.35	0.56	1.00	2.37

4.4 Portfolio results

This part is split into two sections, one for each scenario as described in section 3.5.

4.4.1 Scenario 1

In scenario 1, two portfolio possibilities were presented: the optimal mean-variance portfolio and the optimal Sharpe-ratio portfolio. Figure 9 displays the dispersion of offshore wind in the optimal mean-variance portfolio for scenario 1, where the average power output from 1996-2019 is 8.96 MW and the standard deviation is 3.16 MW.

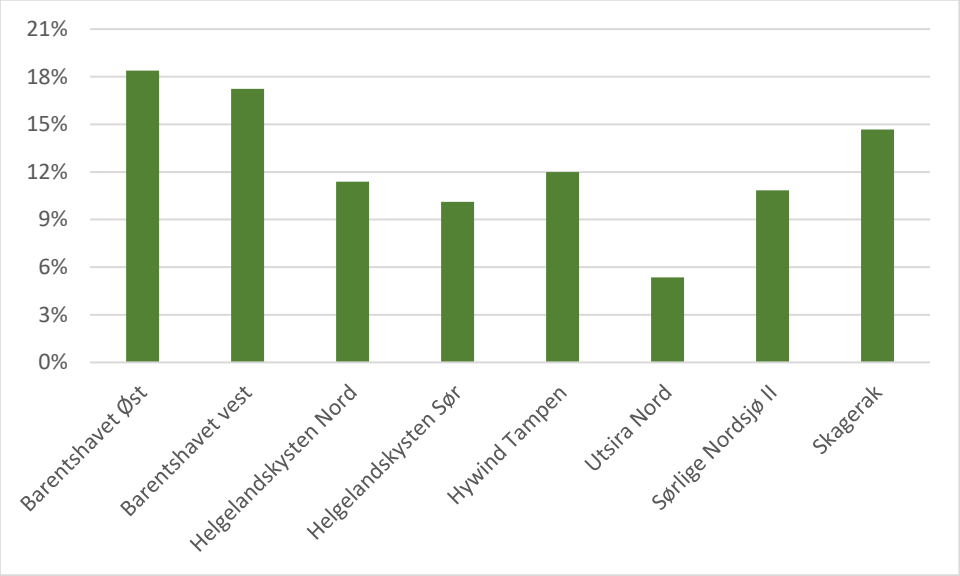

Figure 9: The optimal mean-variance portfolio for scenario 1

The dispersion given by the optimal Sharpe-ratio portfolio for scenario 1 as shown in Figure 10, has a production of 9.04 MW and a standard deviation of 3.17 MW. Thus, resulting in the highest possible Sharpe-ratio of 2.85.

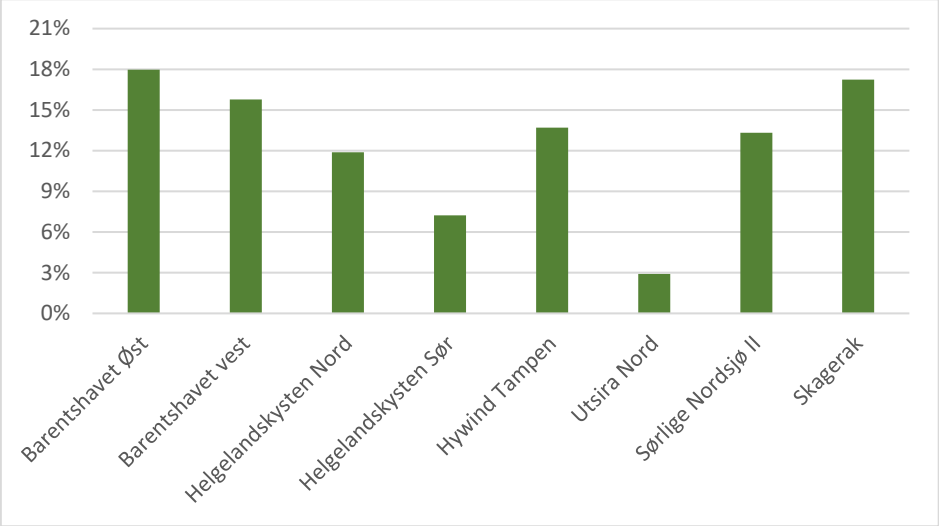

Figure 10: The optimal Sharpe-ratio portfolio for scenario 1

Noticeably, neither portfolio designates any site to have the maximum allowed weight of 25%. The north and south region are the most represented regions in both portfolios, with north being the overall best-scoring region. Barentshavet Øst and Vest are consistently high scorers for both scenarios. West is the overall worst scoring region in both portfolios, mainly caused by Utsira Nord's low scores.

The efficient frontier for scenario 1 is shown in Figure 11. Highlighted are also the portfolios consisting of equal distribution, optimal mean-variance and optimal Sharpe-ratio. Both optimised portfolios are located on the efficient frontier. On the other hand, the equal distribution portfolio have significant lower capacity factor compared to equal risk on the efficient frontier.

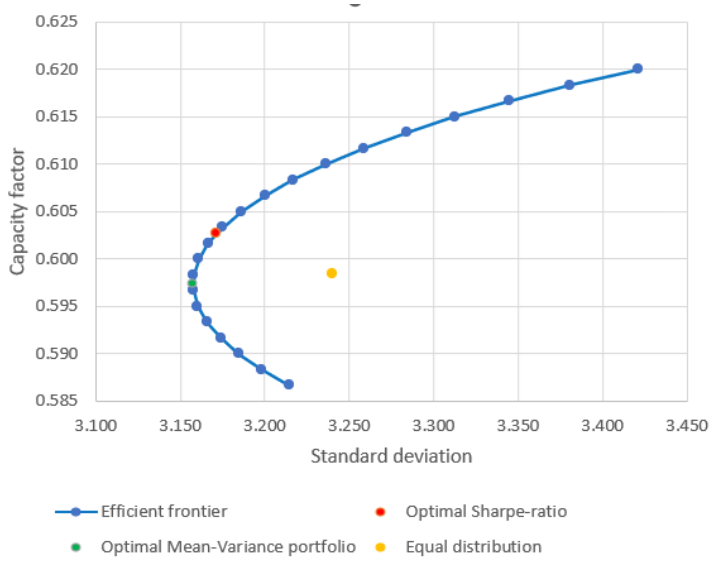

Figure 11: The efficient frontier for scenario 1 with points for equal distribution in all sites, optimal Mean-Variance portfolio and optimal Sharpe-ratio portfolio

4.4.2 Scenario 2

In scenario 2, the portfolio approach was optimised starting with only one site and then adding one site at a time until all eight sites were included in the portfolio. Table 5 shows the results for the mean-variance portfolio for scenario 2. None of the sites are present in the portfolio for all numbers of available sites. Barentshavet Øst appears the most frequent with seven appearances, followed by Skagerak six appearances. Utsira Nord is only included in the portfolio when eight sites are available for selection. The maximum capacity factor of 65.24% is achieved when only one site is selected, while the minimum standard deviation of 3.20 MW occurs when seven out of the eight sites are available for the mean-variance portfolio.

Table 5: Results for the mean-variance portfolio in scenario 2. Shows which sites that are chosen for the number of sites in the portfolio. Standard deviation and capacity factors for each number of sites given.

Scenario 2 Optimal mean-variance								
Number of sites	**1**	**2**	**3**	**4**	**5**	**6**	**7**	**8**
Barentshavet Øst		x	X	x	x	x	x	x
Barentshavet Vest				x	x	x	x	x
Helgelandskysten nord			X		x	x	x	x
Helgelandskysten Sør							x	x
Hywind Tampen				x	x	x	x	x
Utsira Nord								x
Sørlige Nordsjø II	x		X			x	x	x
Skagerak		x		x	x	x	x	x
Standard deviation [MW]	5.89	4.29	3.72	3.48	3.29	3.22	3.20	3.24
Capacity factor [%]	65.24	61.86	60.22	60.38	59.84	60.74	59.87	59.85

The Sharpe-ratio optimisation portfolio for scenario 2 is displayed in Table 6. Neither here, no site is present in the portfolio for every number of sites available. This time however, both Barentshavet Øst and Skagerak is present on seven occasions and Helgelandskysten Nord present on six occasions. Again, Utsira Nord is only included when eight sites are available for selection. Maximum capacity factor is 65.95% and occurs while only one site is chosen. Minimum variability is yet again occurring when seven sites are available, with the same seven sites as in the mean-variance portfolio. However, the highest Sharpe-ratio occurs when six sites are available, with a ratio of 2.83.

Table 6: Results for the Sharpe-ratio portfolio in scenario 2. Shows which sites that are chosen for each number of available sites in the portfolio. Standard deviation, capacity factor and Sharpe-ratio for each number of sites given.

Scenario 2 Optimal Sharpe-ratio								
Number of sites	**1**	**2**	**3**	**4**	**5**	**6**	**7**	**8**
Barentshavet Øst		x	X	x	x	x	x	x
Barentshavet Vest					x	x	x	x
Helgelandskysten nord			X	x	x	x	x	x
Helgelandskysten Sør							x	x
Hywind Tampen				x		x	x	x
Utsira Nord								x
Sørlige Nordsjø II			X		x	x	x	x
Skagerak	x	x		x	x	x	x	x
Standard deviation [MW]	5.92	4.29	3.72	3.50	3.36	3.22	3.20	3.24
Capacity factor [%]	65.95	61.86	60.22	60.78	60.54	60.74	59.87	59.85
Sharpe-ratio	1.67	2.16	2.43	2.61	2.70	2.83	2.80	2.77

In Figure 12 the results of the two portfolios from scenario 2 are plotted alongside the efficient frontier from scenario 1 for comparison. It can be observed that the availability of 6 sites gives the closest result to the efficient frontier for the mean-variance and the Sharpe-ratio portfolio. An availability of 2, 3, 6, 7, and 8 sites yield the same results through the mean-variance and the Sharpe-ratio portfolios. A portfolio consisting of only Utsira Nord and Sørlige Nordsjø II is also visualised to compare the two first large areas designated by the Norwegian government with the portfolio results.

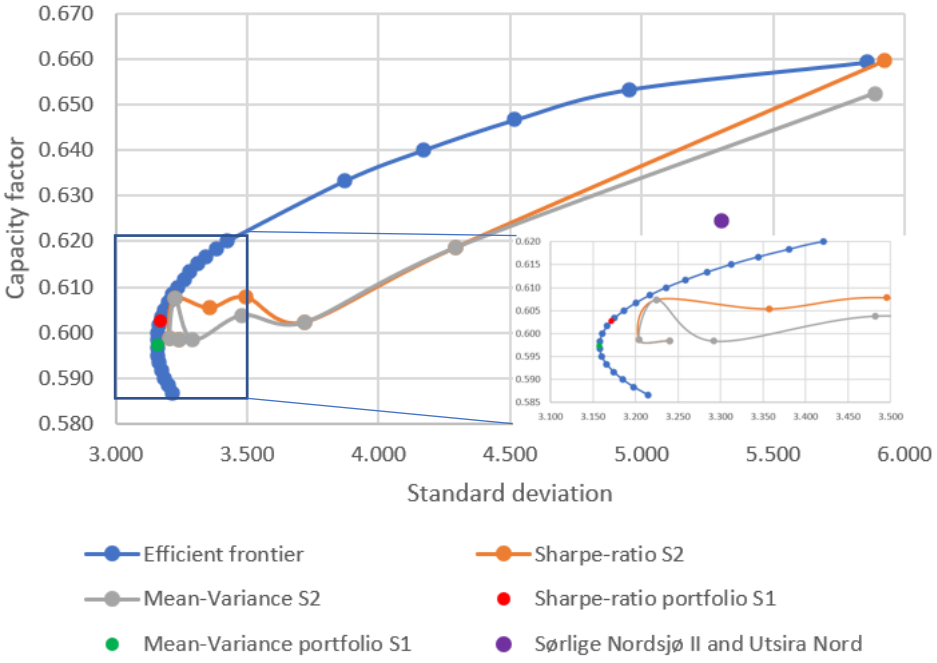

Figure 12: The efficient frontier from scenario 1 with an extension is shown along with the results of the mean-variance and sharpe-ratio portfolios in scenario 2. The sharpe-ratio and mean-variance portfolio for scenario 1 is shown in comparison, along with the portfolio composing of Utsira Nord and Sørlige Nordsjø II.

5 Discussion

Discussion is split into three separate sections. The first section discusses characteristics and the portfolio results. Thereafter a section on model limitations are presented. Lastly, a discussion on how the results from this thesis can be used for further research.

5.1 Offshore wind resources and optimal dispersion of offshore wind power in NEZ

Offshore wind resources in NEZ

In this thesis, a well-verified meteorological hindcast model specific for Norway and its geographical surroundings was utilized. The model revealed that on average basis, NEZ have remarkable wind resources throughout, from north to south. Only 11 percentage points differentiate the capacity factor in the best producing site from the worst, ranging from 55 to 66% before any losses. Sites further offshore is also shown in general terms to have better wind resources. Probably, this is an effect of friction between weather systems and land areas, slowing down the movement of air.

The findings presented in Figure 7 and Figure 8 shows that when integrating several offshore wind sites, power output changes from being skewed towards the extremes for individual sites, to being normally distributed. This finding has important implications for understanding the behaviour of offshore wind energy systems. The fact that the average output distribution appears to be normal suggests that when considered together, the behaviour of the combined power output becomes more predictable and less variable.

As discussed above, existing literature have found that there is a significant decrease in correlation across geographical distance for weather dependent renewable energy. Chapter 4.3 confirms this. Similar to Tande (2022), this thesis finds Stadt to be a geographic barrier for correlation between offshore wind areas in NEZ. However, because this thesis analyse fewer sites than in Tande (2022), it is difficult to determine where the correlation barrier is located due to the distance between analysed sites in mid- and west-NEZ. However, this thesis also finds that there is an even stronger correlation barrier between Helgelandskysten and the Barents Sea. Indicating that a geographical dispersion between these sites gives less variability in production, than a dispersion between Helgelandskysten and the four most southerly sites.

Optimal portfolios scenario 1

The optimal Sharpe-ratio and Mean-variance hourly portfolios are analysed in two scenarios. Both portfolios in scenario 1 diversify across geographic distance. The general notion for both portfolios is the reliance on the most northerly region, thereafter the most southerly region. Specifically, Barentshavet Vest and Øst are allocated more than 15% each for both portfolios. Even though production are generally much lower for the four most northerly sites, they are allocated above 50% in both portfolios. However, they are more present in the mean-variance portfolio than in the Sharpe-ratio portfolio due to the Sharpe-ratio portfolio valuing production. The reliance in both portfolios on the most northern regions could be a hint of the climatological patterns in NEZ. As explained in section 2.3, different parts of NEZ is affected by different weather regimes. The four most southerly sites all experience much of the same weather regimes and systems. This is also indicated through the correlation matrix in Table 4.

The sum of correlation for every site is a useful indicator of the portfolio results. Barentshavet Vest and Øst exhibit significantly lower sum of correlation compared to the other sites. The site with the highest sum of correlation, Utsira Nord, is the least designated site according to the portfolio optimisations. Given that Utsira Nord is one of the two pre-designated areas by the Norwegian government, it may seem like a bit of a surprise at first. However, Utsira Nord have by far the worst wind resources and power output of the four most southerly sites, probably due to its proximity to the Norwegian coastline. It is also located in between the three other sites south of Stadt, making it highly likely to experience the same weather system as at least one of the other sites, at any given moment. Finally, Utsira Nord also have the highest variability (risk) of all sites. Thus, the three other southerly sites inhabiting significant better resources and less variability makes them more suitable according to the portfolio, and thus de-prioritize Utsira Nord.

Both the mean-variance and Sharpe-ratio portfolio is on the efficient frontier, making them both optimal solutions, but with different level of variability and production. Comparing those portfolios to a portfolio of equal distribution between all sites reveal the significance that MPT can bring into spatial energy planning. It is important to note however, that implementing other offshore wind farms in the North Sea from Norway's neighbouring countries probably will skew the portfolio results even more towards the more northerly regions.

Optimal portfolio scenario 2

In scenario 2, a different approach were put forward. Instead of allowing a portfolio to perfectly distribute as it seems fit, equal distribution between the sites were demanded. Both portfolios were optimised for one to eight sites available for development. In both cases, the portfolios start out with a site in the most southern region, followed by a site in the most northern region. When having two or more sites available, one site from the northern and southern region is always chosen in both portfolios. Presumably, this is caused due to those two regions being in each end of NEZ. A site in the mid-region is included when three sites are available but is not selected by the mean-variance portfolio when four sites are available. It is only for 1, 4 and 5 sites available that selection differ between the mean-variance and the Sharpe-ratio portfolio. Therefore, which portfolio approach that are utilized have great importance for the result of selected sites.

There is no order of development that is revealed by this scenario in any of the portfolios due to no site being chosen in all eight instances in neither portfolio. It all depends on how many sites that are available when choosing which sites to develop. However, there are some sites that have more frequent appearances in both portfolios. Barentshavet Øst appears seven times in both portfolios, while Skagerak appears six and seven times in the mean-variance and Sharpe-ratio portfolio, respectively. As discussed above, there seems to be a barrier for correlation at Stadt and between the two most northerly regions. This also shows as both portfolios introduce Helgelandskysten Nord when three sites are available.

The two worst performing sites in scenario 1, Helgelandskysten Sør and Utsira Nord, is respectively selected second to last and last in both portfolios for scenario 2. In the mean-variance portfolio, Sørlige Nordsjø II is seen as the most optimal selection when only one site is available. However, Figure 12 shows that introducing only Utsira Nord to Sørlige Nordsjø II is far from an optimal portfolio given that only two sites are available. It also shows that for both portfolios, going from seven to eight available sites and introducing Utsira Nord, makes the portfolios worse off. In both instances the capacity factor decreases while the variability increases. However, this could be due to the reduction of flexibility for the optimisation model being forced to select all sites in this instance. The possibility to choose more techno-economic areas in NEZ probably would see the result of Utsira Nord's implementation into each portfolio change. Altogether, this might indicate that with a more holistic approach to

energy planning, Utsira Nord might not have been selected this early in Norway's process to develop offshore wind in its economic zone.

5.2 Model limitations and risks

5.2.1 Statistical assumptions

The method used in this thesis relies on the assumption that wind power production follows a normal distribution. Estimated mean, variance, covariance and correlation is calculated based on the data from NORA3-WP. If the power output don't follow a normal distribution, the estimates of these measures may not accurately reflect the true expected returns, risk and correlations between each site selected.

Weather dependent renewable energy like wind power can be affected by unpredictable and non-linear weather patterns that may return volatile power outputs. i.e., if the wind varies just above and below the cut-out speed which leads to more extreme outcomes than a normal distribution will predict. This skewness can lead to estimates of the mentioned measures not reflecting the true relationship between sites selected. Thus, suboptimal portfolio allocations might arise. As presented in section 4.2, each single site's power output do not follow a normal distribution. Thus, uncertainty about the optimal portfolios presented in this thesis arise.

5.2.2 Historical average

NORA3-WP were utilized in this thesis. As mentioned in section 3.1, NORA3-WP is a hindcast model, simulating past weather conditions in the years 1996 to 2019. However, future weather conditions are not going to be equal to past weather conditions. Weather conditions vary from year to year. At the same time, global warming might alter future global wind resources. Global warming increases temperatures unevenly across Earth, generally leading to higher temperature rise the closer an area is towards the poles (Rantanen et al., 2022). Movement of air is caused by pressure differences, which are mainly caused by temperature differences. Smaller temperature differences between equator and the poles will lead to less global wind. According to the Intergovernmental Panel on Climate Change (IPCC), annual global wind speed could drop by up to 10% by 2100 (Robbins, 2022).

5.2.3 Short- and long-range wake-effect

Wind energy is generated by extracting energy from the movement of air. Therefore, the wind downstream of a wind turbine must have a lower velocity compared to the wind in front of the same wind turbine. The downstream wind is the wake of the turbine. Average power

losses in large offshore wind farms are usually in the scale of 10-20% of total power output (Barthelmie et al., 2009). This affects all wind farms, wherever they are built.

Due to offshore wind farms being built larger and to a greater extent in recent years, long-range wake effects between farms have now begun to be evaluated. Stoelinga et al. (2022) found velocity deficits of 10% for distances greater than 100 kilometres from an offshore wind farm. A study from RWE found that the long-range wake effect in some cases can be impactful for more than 200 kilometres. This has not been taken into considerations in this thesis and can change both production and variability. Areas within or close to the North Sea can especially be affected as the surrounding countries aims to have 300 GW installed capacity by 2050 (Henley, 2023).

5.2.4 Weather waiting

Repair and maintenance can only be done in certain climatic conditions. Significant wave heights and unfavourable weather conditions can halt service vessels from doing work on offshore wind farm sites. This situation causing production losses, is called weather waiting. Significant wave height of above three meters constraints all service vessels, while different wind speeds constraint work safety for different operation and maintenance tasks (Gintautas & Sørensen, 2017). NVE (2023) published a map with average wave height for NEZ. This shows different wave conditions throughout and can therefore affect production losses from each site differently. Thus, the results in this thesis might be altered.

5.2.5 Wind turbine Icing

With temperatures below the freezing point and some form of moisture available in the air (clouds, precipitation, snow, sea spray), wind turbines can accumulate ice. This is called wind turbine icing. Research have shown that icing can cause losses beyond 10% of annual energy production (Hansson et al., 2016). Given the meteorological conditions necessary for icing to occur, areas further north are more likely to experience icing, and thus losses in energy production. Knowledge surrounding how much each area would be affected by icing, could alter the results of this thesis.

5.2.6 Cost of offshore wind

The cost perspective is only partially considered through this thesis. As mentioned the non-designated sites selected were done with the research of Solbrekke, I. and Sorteberg, A.

(2022). Only four techno-economic factors were used to evaluate suitability for offshore wind in NEZ. Ocean depth, minimum distance to the Norwegian central electricity network, minimum distance to oil and gas installations, and the risk of desired technology i.e., monopile or floating. These four techno-economic factors will also have different cost profiles than the estimated for future offshore wind, thus the suitability ranking is not static.

Solbrekke, I. and Sorteberg, A. (2022) did not consider all economic factors a developer will consider when deciding if they want to develop an offshore wind farm. Several other economic factors like distances to established infrastructure, logistics, financing and interest, and electricity prices will all be considered. Conclusively, the results of this thesis should be looked at as an evaluation of optimal performance of power production from offshore wind in NEZ and not optimal dispersion by economic standards.

5.3 Further research

A holistic approach to energy planning regarding offshore wind in NEZ will be beneficial. The implementation of large amounts of offshore wind will make the Norwegian energy system more weather dependent. Therefore, minimizing variability in power output is necessary. This thesis have analysed optimal placement of offshore wind in NEZ using hourly data. However, as mentioned in Abelsen (2023), the Norwegian power system will in the future experience variations down to milliseconds due to more variable power inputs. Thus, future work should be done analysing optimal placement using data on shorter timescales than the hourly data this thesis utilized.

One of the flaws of this thesis is that only eight sites were considered. In the view of the stock market, this can be seen as only choosing to evaluate some few assets, instead of the whole market. Therefore, more sites should be evaluated to create a more accurate screening of how to disperse offshore wind in NEZ.

Future research should also include the other variable, weather dependent power producing technologies in NEZ. Such as run-of-river power plants and future installed solar power. To reduce variability into the Norwegian power system, all variable sources of power need to be evaluated in a holistic approach. The effect of transmission restrictions within Norway due to insufficient grid capacity should be within a future analysis. As Norway also have

interconnectors with its neighbouring countries, these could also be considered, along with the variable, weather dependent power producing technologies in those countries.

6 Conclusion

This thesis have analysed the characteristics of eight offshore wind sites, along with the optimal geographical dispersion of offshore wind between these sites through the use of MPT. Capacity factor for all eight sites with IEA's 15 MW reference turbine are between 54.7 to 66% before any losses while the standard deviation ranges from 5.89-6.20 MW. As found by others, this thesis confirms that correlation between areas decrease with geographical distance. A geographical correlation barrier seems to be present around Stadt. However, this thesis also find negligible correlation between areas in the mid and north region, indicating that another geographical barrier for correlation is present somewhere between the sites in those regions.

Both portfolios in scenario 1 distribute across geographical distance, with the northern region being the most designated while the western region is the least designated. No site is designated the maximum allowed amount, showing that geographical dispersion is of importance. Both portfolios in scenario 1 are on the efficient frontier, showing that both are optimal solutions. Average power output are 8.96 and 9.04MW, while the standard deviations are 3.16 and 3.17 MW for the mean-variance and Sharpe-ratio portfolio, respectively. The highest possible Sharpe-ratio were found to be 2.85.

Scenario 2 seems to choose sites with the geographical barrier as a guide, choosing areas in the south, mid and north region first for both portfolios. The result closest to the efficient frontier for the portfolios in scenario 2 is occurring when 6 areas are available, resulting in a capacity factor of 60.74 and a Sharpe-ratio of 2.83 for both. The addition of the already pre-designated area Utsira Nord, makes the portfolios in scenario 2 worse off, while it is the least designated area in scenario 1. This indicates that a more holistic approach to energy planning for offshore wind in NEZ is needed when 30 GW of offshore wind is planned to be allocated to developers within 2040.

7 References

Aasen, M., Klemetsen, M. & Vatn, A. (2022). *Folk og klima: Utvikling i nordmenns oppfatninger om klimaendringer, klimapolitikk og eget ansvar 2018-2021*. Oslo: Cicero.

Abelsen, A. (2023). *Statnett advarer mot systemkollaps*. Energiteknikk. Available at: https://energiteknikk.net/2023/05/statnett-advarer-mot-systemkollaps/ (accessed: 04.05).

Awerbuch, S. & Berger, M. (2003). *Applying Portfolio Theory to EU Electricity Planning and Policy-Making*. Sweden.

Awerbuch, S. (2006). Portfolio-Based Electricity Generation Planning: Policy Implications For Renewables And Energy Security. *Mitigation and Adaptation Strategies for Global Change*, 11 (3): 693-710. doi: 10.1007/s11027-006-4754-4.

Barthelmie, R. J., Hansen, K., Frandsen, S. T., Rathmann, O., Schepers, J. G., Schlez, W., Phillips, J., Rados, K., Zervos, A., Politis, E. S., et al. (2009). Modelling and measuring flow and wind turbine wakes in large wind farms offshore. *Wind Energy*, 12 (5): 431-444. doi: https://doi.org/10.1002/we.348.

Bilgili, M. & Alphan, H. (2022). Global growth in offshore wind turbine technology. *Clean Technologies and Environmental Policy*, 24 (7): 2215-2227. doi: 10.1007/s10098-022-02314-0.

BjerknesCentre. (2020). *Tropiske Sykloner*. Available at: https://bjerknes.uib.no/artikler/faktasider/tropiske-sykloner (accessed: 06.04).

Chang, E. K. M., Lee, S. & Swanson, K. L. (2002). Storm Track Dynamics. *Journal of Climate*, 15 (16): 2163-2183. doi: https://doi.org/10.1175/1520-0442(2002)015<02163:STD>2.0.CO;2.

Clarke, R., de Silva, H. & Thorley, S. (2010). Minimum Variance Portfolio Composition. *The Journal of Portfolio Management*, 37. doi: 10.2139/ssrn.1549949.

Cutululis, N. A. & Sorensen, P. (2010, Oct 18-19). *Simulating Offshore Wind Power Variability over Power Systems Areas*. 9th International Workshop on Large-Scale Integration of Wind Power into Power Systems as well as on Transmission Networks for Offshore Wind Power Plants, Quebec City, CANADA.

deLlano-Paz, F., Calvo-Silvosa, A., Antelo, S. I. & Soares, I. (2017). Energy planning and modern portfolio theory: A review. *Renewable and Sustainable Energy Reviews*, 77: 636-651. doi: https://doi.org/10.1016/j.rser.2017.04.045.

DNV. (2021). *Energy Transition Outlook 2022: A global and regional forecast to 2050*

Drake, B. & Hubacek, K. (2007). What to expect from a greater geographic dispersion of wind farms?—A risk portfolio approach. *Energy Policy*, 35 (8): 3999-4008. doi: https://doi.org/10.1016/j.enpol.2007.01.026.

Energifakta Norge. (2021). *Kraftproduksjon*: Energifakta Norge. Available at: https://energifaktanorge.no/norsk-energiforsyning/kraftforsyningen/ (accessed: 05.05).

Equinor. (2019). *Hywind Tampen - PUD del II - Konsekvensutredning*.

European Commision. (2022). *2030 Climate Target Plan*. climate.ec.europa.eu: European Commision. Available at: https://climate.ec.europa.eu/eu-action/european-green-deal/2030-climate-target-plan_en (accessed: 04.05).

Forskrift om rapportering m.m. av luftfartshinder. (2014). *Forskrift om rapportering, registrering og merking av luftfartshinder*: Lovdata.

Gaertner, E., Rinker, Jennifer., Sethuraman, Latha., Zahle, Frederik., Anderson, Benjamin., Barter, Garrett., Abbas, Nikhar., Meng, Fanzhong., Bortolotti, Pietro., Skrzypinski, Witolt., Scott, George., Feil, Roland., Bredmose, Henrik., Dykes, Katherine., Shields, Matt., Allen, Christopher., Viselli, Anthony. (2020). *Definition of the IEA 15-Megawatt Offshore Referendce Wind*. Golden, CO.

Gaffney, S. J., Robertson, A. W., Smyth, P., Camargo, S. J. & Ghil, M. (2007). Probabilistic clustering of extratropical cyclones using regression mixture models. *Climate Dynamics*, 29 (4): 423-440. doi: 10.1007/s00382-007-0235-z.

Gintautas, T. & Sørensen, J. D. (2017). Improved Methodology of Weather Window Prediction for Offshore Operations Based on Probabilities of Operation Failure. *Journal of Marine Science and Engineering*, 5 (2): 20.

GoogleMaps. (2023). *Distance between two points*. https://www.google.com/maps: Google.

Greatbatch, R. J. (2000). The North Atlantic Oscillation. *Stochastic Environmental Research and Risk Assessment*, 14 (4): 213-242. doi: 10.1007/s004770000047.

Haakenstad, H., Breivik, Ø., Furevik, B. R., Reistad, M., Bohlinger, P. & Aarnes, O. J. (2021). NORA3: A Nonhydrostatic High-Resolution Hindcast of the North Sea, the Norwegian Sea, and the Barents Sea. *Journal of Applied Meteorology and Climatology*, 60 (10): 1443-1464. doi: https://doi.org/10.1175/JAMC-D-21-0029.1.

Hansson, J., Lindvall, J. & Byrkjedal, Ø. (2016). *Quantification of icing losses in wind farms*: Energiforsk.

Henley, J. (2023, 24.04.2023). European countries pledge huge expansion of North Sea wind farms. *The Guardian*. Available at: https://www.theguardian.com/environment/2023/apr/24/european-countries-pledge-huge-expansion-of-north-sea-wind-farms (accessed: 28.04.2023).

Henriksen, M. E., Østenby, A. M. & Skau, S. (2020). *Hva er egentlig potensialet for opprusting og utvidelse av norske vann kraftverk?*

Huber, M., Dimkova, D. & Hamacher, T. (2014). Integration of wind and solar power in Europe: Assessment of flexibility requirements. *Energy*, 69: 236-246. doi: https://doi.org/10.1016/j.energy.2014.02.109.

Hurrell, J. W. & Deser, C. (2010). North Atlantic climate variability: The role of the North Atlantic Oscillation. *Journal of Marine Systems*, 79 (3): 231-244. doi: https://doi.org/10.1016/j.jmarsys.2009.11.002.

IEA. (2021). *Greenhouse Gas Emissions from Energy Data Explorer*: International Energy Agency. Available at: https://www.iea.org/data-and-statistics/data-tools/greenhouse-gas-emissions-from-energy-data-explorer (accessed: 04.05).

IRENA. (2022). *Renewable Power Generation Costs in 2021*. Abu Dhabi: International Renewable Agency.

Jensen, C. U., Panduro, T. E. & Lundhede, T. H. (2014). The Vindication of Don Quixote: The Impact of Noise and Visual Pollution from Wind Turbines. *Land Economics*, 90 (4): 668-682.

Kartverket. (2023a). *Norgeskart*.

Kartverket. (2023b). *Norgeskart*.

Katzenstein, W. & Apt, J. (2012). The cost of wind power variability. *Energy Policy*, 51: 233-243. doi: https://doi.org/10.1016/j.enpol.2012.07.032.

Kautz, L.-A., Martius, O., Pfahl, S., Pinto, J., Ramos, A., Sousa, P. & Woollings, T. (2021). *Atmospheric Blocking and Weather Extremes over the Euro-Atlantic Sector – A Review*.

Kiviluoma, J., Holttinen, H., Weir, D., Scharff, R., Soder, L., Menemenlis, N., Cutululis, N. A., Lopez, I. D., Lannoye, E., Estanqueiro, A., et al. (2016). Variability in large-scale wind power generation. *Wind Energy*, 19 (9): 1649-1665. doi: 10.1002/we.1942.

Koestler, V., Henriksen, M. E., Sidelnikova, M., Veie, C. A., Magnussen, I. H., Hole, J., Wold, M., Haddeland, I., Skaansar, E. & Østenby, A. M. (2020). *Det svinger mer med fornybar strøm: sammenhengende vær i Nord-Europa skaper utfordringer i et fornybart kraftsystem*. Oslo: Norges vassdrag- og energidirektorat

Lockwood, J. G. (1987). ATMOSPHERIC CIRCULATION, GLOBALAtmospheric circulation, global. In *Climatology*, pp. 131-140. Boston, MA: Springer US.

Markowitz, H. (1952). Portfolio Selection. *The Journal of Finance*, 7 (1): 77-91. doi: 10.2307/2975974.

Martin, C. M. S., Lundquist, J. K. & Handschy, M. A. (2015). Variability of interconnected wind plants: correlation length and its dependence on variability time scale. *Environmental Research Letters*, 10 (4). doi: 10.1088/1748-9326/10/4/044004.

Muñoz, J. I., Sánchez de la Nieta, A. A., Contreras, J. & Bernal-Agustín, J. L. (2009). Optimal investment portfolio in renewable energy: The Spanish case. *Energy Policy*, 37 (12): 5273-5284. doi: https://doi.org/10.1016/j.enpol.2009.07.050.
NASA. (2021). *Earth Fact Sheet*. Available at: https://nssdc.gsfc.nasa.gov/planetary/factsheet/earthfact.html (accessed: 17.04).
NVE. (2010). *Havvind - Forslag til utredningsområder*. Oslo: Norges Vassdrags- og Energidirektorat.
NVE. (2012). *Havvind - Strategisk Konsekvensutredning*. Oslo: Norges Vassdrags- og Energidirektorat.
NVE. (2022). *Data for utbygde vindkraftverk i Norge*. NVE.no. Available at: https://www.nve.no/energi/energisystem/vindkraft/data-for-utbygde-vindkraftverk-i-norge/ (accessed: 05.05).
NVE. (2023). *Bølgeforhold*. veiledere.nve.no: NVE. Available at: https://veiledere.nve.no/havvind/identifisering-av-utredningsomrader-for-havvind/teknologi-kraftsystem-og-lovverk/fysiske-forhold/bolgeforhold/ (accessed: 29.04).
Ólafsdóttir, R. & Sæþórsdóttir, A. D. (2019). Wind farms in the Icelandic highlands: Attitudes of local residents and tourism service providers. *Land Use Policy*, 88: 104173. doi: https://doi.org/10.1016/j.landusepol.2019.104173.
OSSfoundation. (2014). *North Atlantic Oscillation (NAO)*. Available at: https://ossfoundation.us/projects/environment/global-warming/north-atlantic-oscillation-nao?searchterm=north+atlantic+oscil (accessed: 06.04).
Rand, J. & Hoen, B. (2017). Thirty years of North American wind energy acceptance research: What have we learned? *Energy Research & Social Science*, 29: 135-148. doi: https://doi.org/10.1016/j.erss.2017.05.019.
Rantanen, M., Karpechko, A. Y., Lipponen, A., Nordling, K., Hyvärinen, O., Ruosteenoja, K., Vihma, T. & Laaksonen, A. (2022). The Arctic has warmed nearly four times faster than the globe since 1979. *Communications Earth & Environment*, 3 (1): 168. doi: 10.1038/s43247-022-00498-3.
Regjeringen. (2022a). *Høringsnotat om tildeling av fase én av Sørlige Nordsjø II*. Energy, M. o. P. a.
Regjeringen. (2022b). *Høringsnotat om tildeling av områdene i Utsira Nord*. Energy, M. o. P. a.
Regjeringen. (2022c). *Kraftfull satsing på havvind*. Regjeringen.no: Regjeringen.
Regjeringen. (2022d). *Nytt norsk klimamål på minst 55 prosent*. Regjeringen.no. Available at: https://www.regjeringen.no/no/aktuelt/nytt-norsk-klimamal-pa-minst-55-prosent/id2944876/ (accessed: 03.05).
Reichenberg, L., Wojciechowski, A., Hedenus, F. & Johnsson, F. (2017). Geographic aggregation of wind power—an optimization methodology for avoiding low outputs. *Wind Energy*, 20 (1): 19-32. doi: https://doi.org/10.1002/we.1987.
Robbins, J. (2022). *Global 'Stilling': Is Climate Change Slowing Down the Wind?* : Yale Environment 360. Available at: https://e360.yale.edu/features/global-stilling-is-climate-change-slowing-the-worlds-wind (accessed: 12.05).
Rombauts, Y., Delarue, E. & D'haeseleer, W. (2011). Optimal portfolio-theory-based allocation of wind power: Taking into account cross-border transmission-capacity constraints. *Renewable Energy*, 36 (9): 2374-2387. doi: https://doi.org/10.1016/j.renene.2011.02.010.
Roques, F., Hiroux, C. & Saguan, M. (2010). Optimal wind power deployment in Europe—A portfolio approach. *Energy Policy*, 38 (7): 3245-3256. doi: https://doi.org/10.1016/j.enpol.2009.07.048.
Schultz, D. M. & Vaughan, G. (2011). Occluded Fronts and the Occlusion Process: A Fresh Look at Conventional Wisdom. *Bulletin of the American Meteorological Society*, 92 (4): 443-466. doi: https://doi.org/10.1175/2010BAMS3057.1.
Sharpe, W. F. (1963). A Simplified Model for Portfolio Analysis. *Management Science*, 9 (2): 277-293.
Smirnova, J. E., Golubkin, P. A., Bobylev, L. P., Zabolotskikh, E. V. & Chapron, B. (2015). Polar low climatology over the Nordic and Barents seas based on satellite passive microwave data. *Geophysical Research Letters*, 42 (13): 5603-5609. doi: https://doi.org/10.1002/2015GL063865.

Solbrekke, I., Sorteberg, A. & Haakenstad, H. (2021). The 3 km Norwegian reanalysis (NORA3) – a validation of offshore wind resources in the North Sea and the Norwegian Sea. *Wind Energy Science*, 6: 1501-1519. doi: 10.5194/wes-6-1501-2021.

Solbrekke, I. & Sorteberg, A. (2022). *Offshore Wind Farm Siting -Suitability Scores for the Norwegian Economic Zone Using Multi-Criteria Decision Analysis*.

Solbrekke, I. M., Kvamstø, N. G. & Sorteberg, A. (2020). Mitigation of offshore wind power intermittency by interconnection of production sites. *Wind Energ. Sci.*, 5 (4): 1663-1678. doi: 10.5194/wes-5-1663-2020.

Solbrekke, I. M. & Sorteberg, A. (2022). NORA3-WP: A high-resolution offshore wind power dataset for the Baltic, North, Norwegian, and Barents Seas. *Scientific Data*, 9 (1). doi: 10.1038/s41597-022-01451-x.

Statnett. (2022a). *Det eksepsjonelle kraftåret 2021*: Statnett. Available at: https://www.statnett.no/om-statnett/nyheter-og-pressemeldinger/nyhetsarkiv-2022/det-eksepsjonelle-kraftaret-2021/ (accessed: 05.05).

Statnett. (2022b). *Kortsiktig Markedsanalyse 2022-27*: Statnett.

Statnett. (2023). *Forbruksutvikling i Norge 2022-2050 - delrapport til Langsiktig Markedsanalyse 2022-2050*: Statnett.

Stoelinga, M., Sanchez-Gomez, M., S. Poulos, G. & Crescenti, J. (2022). *Estimating Long-Range External Wake Losses in Energy Yield and Operational Performance Assessments Using the WRF Wind Farm Parameterization*.

Tande, J. O. G. (2022). *Ulike vindforhold: Slik bør vi bygge 30 GW havvind i Norge*, 2023, 15.08: Sintef.

UNEP. (2022). *Emissions Gap Report 2022: The Closing Window: Climate crisis calls for rapid transformation of societies*. Kenya: UNEP.

van der Wiel, K., Bloomfield, H., Lee, R., Stoop, L., Blackport, R., Screen, J. & Selten, F. (2019). The influence of weather regimes on European renewable energy production and demand. *Environmental Research Letters*. doi: 10.1088/1748-9326/ab38d3.

Wanner, H., Brönnimann, S., Casty, C., Gyalistras, D., Luterbacher, J., Schmutz, C., Stephenson, D. B. & Xoplaki, E. (2001). North Atlantic Oscillation – Concepts And Studies. *Surveys in Geophysics*, 22 (4): 321-381. doi: 10.1023/A:1014217317898.

White Consultants. (2020). *Review and Update of Seascape and Visual Buffer study for Offshore Wind farms*.

World Bank. (2019). *Going Global : Expanding Offshore Wind To Emerging Markets*. Washington, D.C: World Bank Group.

8 Appendix

Appendix A

```
import xarray as xr
import numpy as np

# Open the NC-file
nc_file = xr.open_dataset("D:\Havvind - data fra
modell\WindPower_capacity_factor_monthly.nc")

# Extract the relevant variables
lon = nc_file["lon"].values
lat = nc_file["lat"].values

# Define the target longitude and latitude
target_lon = 4.51583
target_lat = 59.26194

# Calculate the distances between the target and all points
dists = np.sqrt((lon - target_lon)**2 + (lat - target_lat)**2)

# Find the indices of the closest match
y_index, x_index = np.unravel_index(dists.argmin(), dists.shape)

# Print the result
print("The indices x_index: ", x_index, " and y_index: ", y_index, "
correspond to lon: ", lon[y_index, x_index], " and lat: ", lat[y_index,
x_index])
```

Appendix B

```
import xarray as xr

# Open the NC-file
nc_file = xr.open_dataset("D:\Havvind - data fra
modell\WindPower_capacity_factor_monthly.nc")

# Extract the relevant variables
lon = nc_file["lon"].values
lat = nc_file["lat"].values

# Define the target X and Y indices
target_y = 229
target_x = 507

# Find the corresponding latitude and longitude
target_lat = lat[target_x, target_y]
target_lon = lon[target_x, target_y]

# Print the result
print("Y index: ", target_y, " and X index: ", target_x, " correspond to
lat: ", target_lat, " and lon: ", target_lon)
```

Appendix C

```
% Load the file
file_path = 'D:\Kjøring i matlab\cat_4_5.mat';
if exist(file_path, 'file')
    load(file_path);
else
    error('File not found!');
end

% Create a binary image from the matrix
img = double(~isnan(ind_rob));

% Create a colormap with white for NaN values and blue for 1 values
colormap([1 1 1; 0 0 1]);

% Display the image
imagesc(ind_rob);

% Set the axis labels
xlabel('X');
ylabel('Y');

% Add an interactive data cursor to show the coordinates of each 1 value
dcm = datacursormode(gcf);
set(dcm, 'UpdateFcn', @(obj, event_obj) sprintf('X: %.0f, Y: %.0f',
event_obj.Position(1), event_obj.Position(2)));

% Add grid for every 50th value in X and Y directions
grid_step = 50;
x_ticks = 1:grid_step:size(ind_rob, 2);
y_ticks = 1:grid_step:size(ind_rob, 1);
set(gca, 'XTick', x_ticks, 'YTick', y_ticks, 'GridLineStyle', '-', 'XMinorTick',
'on', 'YMinorTick', 'on', 'XAxisLocation', 'top', 'YDir', 'reverse', 'Layer',
'top');
grid on;
```

Appendix D

```
import matplotlib.pyplot as plt
import cartopy.crs as ccrs
import cartopy.feature as cfeature
import numpy as np

# Define the coordinates to highlight

lats1 = [56.823333, 57.093333, 56.738056, 56.591667, 56.483889]
lons1 = [4.346667, 5.168056, 5.4975, 5.033611, 4.641389]
lats2 = [61.38821, 61.30250, 61.27735, 61.36306]
lons2 = [2.26150, 2.30803, 2.26169, 2.21516]
lats3 = [59.448056, 59.482222, 59.105000, 59.069444]
lons3 = [4.269167, 4.673611, 4.812222, 4.407500]

# Define the coordinates of the point to plot
#SNII
point_lat1 = 56.7832348923
point_lon1 = 4.899644786
#UN
point_lat2 = 59.293864
point_lon2 = 4.536812
```

```
#skagerak
point_lat3 = 57.389502
point_lon3 = 7.415621
#Hywind Tampen:
point_lat4 = 61.3338919
point_lon4 = 2.25502306
#Barentshavet vest:
point_lat5 = 71.844295
point_lon5 = 22.071612
#Barentshavet øst
point_lat6 = 71.898925
point_lon6 = 32.228565
#Helgelandskysten nord
point_lat7 = 66.716214
point_lon7 = 10.028735
#helgelandskysten sør
point_lat8 = 64.664145
point_lon8 = 9.450846

# Create a figure and an axes object
fig = plt.figure(figsize=(10, 10))
ax = fig.add_subplot(1, 1, 1, projection=ccrs.Mercator())

# Set the extent of the map to cover the North Sea region
ax.set_extent([0, 33, 56, 73], crs=ccrs.PlateCarree())

# Add coastlines, countries, and states
ax.add_feature(cfeature.COASTLINE)
ax.add_feature(cfeature.BORDERS, linestyle='-', edgecolor='gray')
ax.add_feature(cfeature.STATES, linestyle='-', edgecolor='gray')

# Draw a polygon to highlight the area
ax.fill(np.asarray(lons1), np.asarray(lats1), transform=ccrs.PlateCarree(),
alpha=0.3, color='red')
ax.fill(np.asarray(lons2), np.asarray(lats2), transform=ccrs.PlateCarree(),
alpha=0.3, color='red')
ax.fill(np.asarray(lons3), np.asarray(lats3), transform=ccrs.PlateCarree(),
alpha=0.3, color='red')

# Add land, ocean, and rivers
ax.add_feature(cfeature.LAND, facecolor='gray', edgecolor='none')
ax.add_feature(cfeature.OCEAN, facecolor='aqua', edgecolor='none')
ax.add_feature(cfeature.RIVERS)

# Add a red diamond for the specified point
ax.plot(point_lon1, point_lat1, 'D', markersize=2,
transform=ccrs.PlateCarree(), color='red')
ax.plot(point_lon2, point_lat2, 'D', markersize=2,
transform=ccrs.PlateCarree(), color='red')
ax.plot(point_lon3, point_lat3, 'D', markersize=2,
transform=ccrs.PlateCarree(), color='red')
ax.plot(point_lon4, point_lat4, 'D', markersize=2,
transform=ccrs.PlateCarree(), color='red')
ax.plot(point_lon5, point_lat5, 'D', markersize=2,
transform=ccrs.PlateCarree(), color='red')
ax.plot(point_lon6, point_lat6, 'D', markersize=2,
transform=ccrs.PlateCarree(), color='red')
ax.plot(point_lon7, point_lat7, 'D', markersize=2,
transform=ccrs.PlateCarree(), color='red')
ax.plot(point_lon8, point_lat8, 'D', markersize=2,
transform=ccrs.PlateCarree(), color='red')
```

```
# Define the labels for the points
labels = ['SNII', 'UN', 'Skagerak', 'Hywind Tampen', 'Barentshavet vest',
'Barentshavet øst', 'Helgelandskysten nord', 'Helgelandskysten sør']

# Add the labels to the plot
ax.text(point_lon1, point_lat1, labels[0], fontsize=5,
transform=ccrs.PlateCarree(), color='black', va='bottom', ha='left')
ax.text(point_lon2, point_lat2, labels[1], fontsize=5,
transform=ccrs.PlateCarree(), color='black', va='bottom', ha='right')
ax.text(point_lon3, point_lat3, labels[2], fontsize=5,
transform=ccrs.PlateCarree(), color='black', va='bottom', ha='right')
ax.text(point_lon4, point_lat4, labels[3], fontsize=5,
transform=ccrs.PlateCarree(), color='black', va='bottom', ha='center')
ax.text(point_lon5, point_lat5, labels[4], fontsize=5,
transform=ccrs.PlateCarree(), color='black', va='bottom', ha='right')
ax.text(point_lon6, point_lat6, labels[5], fontsize=5,
transform=ccrs.PlateCarree(), color='black', va='bottom', ha='right')
ax.text(point_lon7, point_lat7, labels[6], fontsize=5,
transform=ccrs.PlateCarree(), color='black', va='bottom', ha='right')
ax.text(point_lon8, point_lat8, labels[7], fontsize=5,
transform=ccrs.PlateCarree(), color='black', va='bottom', ha='right')


# Show the map
plt.show()
```

Appendix E

```
import xarray as xr
import pandas as pd
import glob2
import os

# Define the folder path and name pattern
folder_path = "D:\Havvind - data fra modell\Hourly data"
file_pattern = "WindPower_generation_hourly_*.nc"

# Use glob2 to find all matching files in the folder
file_paths = sorted(glob2.glob(os.path.join(folder_path, file_pattern)))

# Initialize an empty list to store the dataframes
dfs = []

# Loop over all the files and extract the relevant data
for file_path in file_paths:
    ds = xr.open_mfdataset(file_path, decode_times=False)
    lon = ds["lon"].values
    lat = ds["lat"].values
    y_idx = 311  # Index of the desired X value
    x_idx = 477  # Index of the desired Y value
    ds = ds.isel(X=y_idx, Y=x_idx, Z=2)
    hourly_generation = ds["WindPower_generation_hourly"].values[:, 0, 2]
    times = pd.to_datetime(ds["time"].values)
    df = pd.DataFrame({'time': times, 'power_generation':
hourly_generation}
)
    dfs.append(df)
```

```
# Check if the Excel file exists
try:
    existing_df = pd.read_excel('Produksjon_UN.xlsx')
except FileNotFoundError:
    existing_df = None

# Concatenate the existing dataframe with the new dataframes, if it exists
if existing_df is not None:
    df = pd.concat([existing_df] + dfs, axis=0, ignore_index=True)
else:
    df = pd.concat(dfs, axis=0, ignore_index=True)

# Export the dataframe to an Excel file
df.to_excel('Produksjon_UN.xlsx', index=False)
```

Appendix F

```
import xarray as xr
import pandas as pd
import glob2
import os

# Define the folder path and name pattern
folder_path = "D:\Havvind - data fra modell"
file_pattern = "WindSpeed_monthl*.nc"

# Use glob2 to find all matching files in the folder
file_paths = sorted(glob2.glob(os.path.join(folder_path, file_pattern)))

# Initialize an empty list to store the dataframes
dfs = []

# Loop over all the files and extract the relevant data
for file_path in file_paths:
    ds = xr.open_mfdataset(file_path, decode_times=False)
    lon = ds["lon"].values
    lat = ds["lat"].values
    y_idx = 124  # Index of the desired X value
    x_idx = 978  # Index of the desired Y value
    ds = ds.isel(X=y_idx, Y=x_idx, Z=2)
    hourly_generation = ds["WindSpeed_monthly"].values[:, 0, 2]
    times = pd.to_datetime(ds["time"].values)
    df = pd.DataFrame({'time': times, 'windspeed': hourly_generation})
    dfs.append(df)

# Check if the Excel file exists
try:
    existing_df = pd.read_excel('Vindhastighet_bv.xlsx')
except FileNotFoundError:
    existing_df = None

# Concatenate the existing dataframe with the new dataframes, if it exists
if existing_df is not None:
    df = pd.concat([existing_df] + dfs, axis=0, ignore_index=True)
else:
    df = pd.concat(dfs, axis=0, ignore_index=True)

# Export the dataframe to an Excel file
df.to_excel('Vindhastighet_bv.xlsx', index=False)
```

Appendix G

Table 7: Covariance matrix for every area in this thesis

	BØ	BV	HN	HS	HT	UN	SNII	SG
Barentshavet Øst (BØ)	36.50	11.43	3.41	2.92	1.91	1.42	1.34	1.06
Barentshavet Vest (BV)	11.43	37.40	4.90	3.56	1.60	0.81	1.06	1.05
Helgelandskysten Nord (HN)	3.41	4.90	37.44	20.97	8.12	5.78	3.17	3.29
Helgelandskysten Sør (HS)	2.92	3.56	20.97	37.99	9.31	6.70	3.78	4.78
Hywind Tampen (HT)	1.91	1.60	8.12	9.31	37.95	18.11	9.23	6.48
Utsira Nord (UN)	1.42	0.81	5.78	6.70	18.11	38.44	19.66	12.72
Sørlige Nordsjø II (SNII)	1.34	1.06	3.17	3.78	9.23	19.66	34.66	19.62
Skagerak (SG)	1.06	1.05	3.29	4.78	6.48	12.72	19.62	35.09

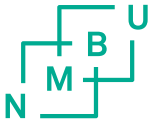

Norges miljø- og biovitenskapelige universitet
Noregs miljø- og biovitskapelege universitet
Norwegian University of Life Sciences

Postboks 5003
NO-1432 Ås
Norway